جامعة أبو بكر بلقايد
UNIVERSITÉ DE TLEMCEN

Pan African University
Institute of Water
and Energy Sciences

Institute of Water and Energy Sciences (Including Climate Change)

DYNAMIC MODELING AND ECONOMIC ANALYSIS AND OPTIMISATION OF PHOTOVOLTAIC GROUND WATER PUMPING SYSTEM FOR IRRIGATION IN HOT ARID CLIMATE

Hillary Kiprono Kipkemoi

Date: 06/09/2017

*Master in **Energy, Engineering track***

President: Prof. Issakha Youm

Supervisor: Prof. Donatien Njomo

External Examiner: Prof. Cherif Ould Lahoucine

Internal Examiner: Dr. Abdellah Benyoucef

Academic Year: 2016-2017

Declaration

I **HILLARY KIPKEMOI KIPRONO** hereby declare that this thesis represents my personal work, realized to the best of my knowledge. I also declare that all information, material and results from other works presented here, have been fully cited and referenced in accordance with the academic rules and ethics.

Name KIPRONO HILLARY KIPKEMOI

Date 06/09/2017…………………

Signature …………………

I am submitting this thesis for examination with the approval of my supervisor:

Name KIPRONO HILLARY KIPKEMOI

Date 06/09/2017…………………

Signature …………………

Supervisors Name PROFESSOR DONATIEN NJOMO

Date …08 / 24 / 2017………………

Signature … ………………

Abstract

Remote areas do not have access to electricity and therefore mostly use diesel water pumping systems (DWPS) to irrigate their crops. It has been, however, found to be expensive and unsustainable in the long run especially to the environment. A good alternative to replace the DWPS in remote areas with low or no access to the grid is the solar water pumping systems (SWPS) particularly for food production. Solar Powered Irrigation Systems (SPIS) performance is affected by environmental conditions that determine the crop water requirements and the solar intensity influencing the production by PV arrays, which exhibit temporal variability. The aim of the study was to design a system for irrigation of maize in hot arid areas. CROPWAT is used to determine the irrigation water requirement necessary for the preliminary design of the system while PVSYST provides the optimal orientation of the PV array. A dynamic modelling of the system is used to assess its performance over the growing period of maize, a Kenyan staple food grain. The water demand was found to be higher in the hot arid areas having peak irrigation requirement of 96.8 m^3 and resulted in a slightly bigger system with its performance varying during the growing season. From the economic feasibility of the system evaluated it was found that the SPIS had higher initial costs, but was cost effective and more profitable to run in the long run. The cost of the energy generation system accounted for 43% of the initial capital costs (ICC) in SPIS as compared to 23% in DPIS. Both systems had nearly the same internal rate of return (IRR) with externality costs not accounted for. SPIS is feasible for deployment in hot arid climate and is expected to provide an alternative and help the semi-arid and arid areas cope with the dangers of food insecurity caused by reliance on unreliable rainfall for farming.

Keywords: Water pumping; Irrigation; Solar pump; Dynamic modelling; performance; arid areas; Economic analysis

Résumé

Les zones éloignées n'ont pas accès à l'électricité et, par conséquent, utilisent principalement des systèmes de pompage d'eau diesel (DWPS) pour irriguer leurs cultures. Cependant, il a été qu'ils sont coûteux et non durables à long terme, en particulier pour l'environnement. Une bonne alternative pour remplacer les DWPS dans des zones éloignées avec peu ou pas d'accès au réseau électrique sont les systèmes de pompage d'eau solaire (SWPS) en particulier pour la production de cultures vivrières. Les performances des systèmes d'irrigation par énergie solaire (SPIS) sont affectées par les conditions environnementales qui déterminent les besoins en eau de la récolte et l'intensité solaire influençant la production d'énergie par les systèmes photovoltaïques, qui présente une variabilité temporelle. Le but de l'étude était de concevoir un système d'irrigation du maïs dans les zones arides chaudes. CROPWAT est utilisé pour déterminer les besoins en eau d'irrigation nécessaires à la conception préliminaire du système, tandis que PVSYST fournit l'orientation optimale du réseau photovoltaïque. Une modélisation dynamique du système est utilisée pour évaluer ses performances sur la période de croissance du maïs, un aliment de base en grain du Kenya. On a constaté que la demande d'eau était plus élevée dans les zones arides chaudes ayant une demande d'irrigation maximale de 96.8 m^3 et ceci a nécessité un système légèrement plus grand avec des performances variant pendant la saison de croissance. D'après la faisabilité économique du système évalué, il a été constaté que le SPIS avait des coûts initiaux plus élevés, mais qu'il était rentable et plus rentable de le faire fonctionner à long terme. Le coût du système de production d'énergie a représenté 43% des coûts initiaux en capital (ICC) dans le SPIS contre 23% pour le DPIS. Les deux systèmes avaient presque le même taux de rendement interne (IRR) lorsque les coûts d'externalité ne sont pas comptabilisés. Le déploiement du SPIS est faisable dans un climat aride et chaud et devrait fournir une alternative et aider les zones semi-arides et arides à faire face aux dangers de l'insécurité alimentaire causés par la dépendance à des précipitations peu fiables pour l'agriculture.

Mots-clés : Pompage de l'eau ; Irrigation ; Pompe solaire ; Modélisation dynamique ; performance; zones arides ; Analyse économique

Acknowledgment

I would like to appreciate the role played by my supervisor Prof. Donatien Njomo in guiding me in the course of this research. His presence was unwavering in providing guidelines while also allowing the research to be my own work.

I would also like to thank the Rural Electrification Authority, (REA) who attached me to their institution to help me carry out this master thesis project. Through their institution and employees, I gained invaluable knowledge and insight into processes that guided this thesis.

The sponsors and GIZ, KFW and the AU for making the programme a success in collaboration with the university, Pan African University Institute of Water and Energy Sciences (PAUWES) that gave me the opportunity to empower myself to be able to solve the continent's problems.

Finally, I would like to give big thanks to my family, for giving me their support since I embarked on this programme. God will bless you abundantly.

TABLE OF CONTENTS

List of Tables

List of Figures

List of abbreviations

C_B	Battery Capacity
E_h	Hydraulic energy
E_L	Daily Energy Load Demand
E_g	Energy generated
H_{LOL}	Hours of Loss of Load
H_{OT}	Hours of Operation
H_{TE}	Total head
I_b	Beam radiation
I_d	Diffuse radiation
I_{dh}	Diffuse horizontal radiation
I_{gh}	Global horizontal radiation
I_r	Reflected radiation
I_t	Total radiation
K_C	Cultural coefficient
N_D	Autonomy Days
P_{eff}	Effective Precipitation
P_{load}	Demand during Power Loss
P_{max}	Peak power from PV array
P_{pv}	Power from the Photovoltaic array
P_{ref}	PV array nominal power
R_n	Daily net radiation on surface of crop
S_f	Safety factor
T_C	Solar cell Temperature
T_a	Ambient temperature
T_{ref}	Solar cell reference temperature
V_B	Battery voltage
V_b	Volume of beneficial water used
V_r	Volume of water stored in the crop root zone
V_s	Volume of water supplied
V_t	Volume of water conveyed to the field
α	Cell temperature coefficient
β	slope of the surface on which the solar array is installed
e_a	Actual vapour pressure
e_s	Saturation vapour pressure
u_2	Wind speed
γ	surface azimuth angle
γ	the psychometric constant
γ_s	solar azimuth angle
ρ	Density of water
η	Solar cell efficiency
η_B	Battery efficiency
η_{CO}	Water conveyance efficiency
η_O	Overall irrigation efficiency
η_a	Water application efficiency
η_i	Irrigation efficiency
η_{inv}	Inverter efficiency
η_{ref}	Solar cell reference efficiency
η_s	System efficiency
θ_z	Zenith angle
Δ	Slope of the vapour pressure curve
A	Area of PV array
AC	Alternating Current
AHP	Analytical Hierarchy Process
AL	Autonomy Level
ANFIS	Adaptive neuro-fuzzy interference system
ANN	Artificial Neural Networks
CF	Cash Flows

CRF	Capital Recovery Factor
CWR	Crop Water Requirement
DC	Direct Current
DE	Periodic Power Loss
DOD	Depth of Discharge
ET_0	reference evapotranspiration
FAO	Food and Agriculture Organization
FOTRAN	Formula Translator
g	Acceleration due to gravity
G	soil heat flux density
GA	Genetic Algorithm
HOMER	Hybrid Optimization Model for Electric Renewables
I	Mean daily radiation on array
IC	Installation Cost
ICC	Initial Capital Cost
iHOGA	improved Hybrid Optimization by Genetic Algorithm
IRR	Internal Rate of Return
IWR	irrigation water requirement
kWh	Kilowatt-hour
LCC	Life Cycle Cost
LCOE	Levelized Cost of Electricity
LD	Load Demand
LOLP	Loss of Load Probability
LPG	Liquefied Petroleum Gas
LPS	Loss of Power Supply
LPSP	Loss of Power Supply Probability
LR	Leaching Reequipment
MATLAB	Matrix Laboratory
MPP	Maximum Power Point
MPPT	Maximum Power Point Tracker
NASA	National Space Agency
NPV	Net Present Value
NREL	National Renewable Energy Laboratory
PBT	Payback time
PMC	Pollution Mitigation Cost
PROMETHEE	Preference Ranking Organization Method for Enrichment Evaluation
PSH	Peak Solar Hours
PV	Photovoltaic
Q	Volume of water pumped daily
RC	Replacement Cost
REA	Rural Electrification Authority
SAPV	Standalone Photovoltaic
SPVWPS	Solar Photovoltaic Pumping Systems
SV	Salvage Value
T	Daily mean air temperature
t	Periodic time under consideration
TEL	Total Energy Loss
TOPSIS	Technique for Ordre Preference by Similarity to Ideal Solution
TRNSYS	Transient System Simulation tool
USD	United States Dollar
W	Watts
WR	Daily water requirement
$NOCT$	Nominal operating cell temperature
$O\&MC$	Operation and Maintenance Cost

CHAPTER ONE: INTRODUCTION

1.1 STUDY OBJECTIVES

Agriculture is responsible for utilization of about 70% of the global fresh water (FAO, 2015). While this may be the case, most of the farmlands are mostly under rain fed agriculture with sub-Saharan Africa having 95% of its farmlands depending on the rain. Together with South Asia, sub-Saharan Africa is suffering from food insecurity due to the low productivity of these practices (IWMI, 2010). In a globe where the dominant employer is agriculture for the over 40% of the population, increase in farm productivities has a positive impact on the livelihoods of this share (IRENA, 2016a).

One of the ways fronted for increasing the productivities of the farms is through efficient irrigation practices. According to FAO, the total farmlands under irrigation is 20% but contributes 40% of the bread basket. The world population is increasing, and at the current rate, the farms will need to produce 60% more by 2050 (FAO, 2015). Regions with semi-arid and arid climates contribute the highest share of land under irrigation. The low share of irrigated land in sub Saharan Africa can, however, be attributed to infrastructural constraints. Factoring in water availability and resource potential, it is predicted that a further 20% more of land will be brought under irrigation by 2030 (UNESCO, 2013).

The water used in irrigation, whether from aquifers, rivers, lakes or reservoirs, requires energy to be distributed in the land. For some fields in which the source is at a higher elevation than the land under irrigation, potential energy will distribute the water in the farm. However, in the future scenario, groundwater from shallow aquifers has been projected to play an important role especially in arid and semi-arid lands (UNESCO, 2013).

Currently, 56% of the land under irrigation requires energy. The use of fossil fuels to supply the energy is unsustainable due to the externalities of greenhouse gas emissions coupled with the cumbersome nature of the transportation of the fuel in remote areas. A local solution that is clean, sustainable and cost effective is, therefore, the prerequisite in solving small scale irrigation, especially in the developing countries. Solar energy shows great potential for utilization in countries like Kenya with a high amount of solar insolation. This adds to the advantage that the water requirement varies almost linearly with the increased amount of solar insolation (Anis & Metwally, 1994; Reddy, 2014).

Semi-arid and arid regions have less surface water resources and therefore ground water sources have served as the main source of irrigation water. The current state of exploitation is 10% of the irrigation potential, and if 50% were to be developed, it would not only make Kenya food secure, it would also make it an exporter (Ngigi, 2002). Pumping the water, however, requires significant amounts of energy which have always been met using diesel pumps.

The main challenge in the deployment of solar water pumps for irrigation has been the high initial cost of the various components. Thus, optimization of the components that make the system reliable and reduce oversizing hence increased capital costs is a good alternative. Mainstream designs have been about designing the systems separately without taking into consideration the fact that the IWR and solar energy harnessed are both affected by the environmental conditions. A new approach that integrates the whole system and the transient effects of the environmental conditions on the IWR and solar energy harnessed is proposed. This not only ensures there is a sustainable use of the scarce water resources but also brings to the fore the reduction in the overall cost of the system.

Irrigation in hot climates provides a rather peculiar problem especially in using SAPV systems. The high temperatures result in higher evapotranspiration rates as well as a reduction in the efficiency of the PV arrays. According to Hasan et al. (Hasan, Mccormack, Huang, and Norton, 2014), the operating temperature of a PV panel is largely dependent on the local climatic conditions attaining 50% and 80% of incident irradiation reaching the solar panels in Germany and in Sudan respectively. Thus, the operating temperature and the power loss due to temperature effect is different for the two locations.

1.1.1 Research Gap

Research has been done in the area of solar water pumping for irrigation purposes in remote areas due to their impact on increasing productivity of the lands (FAO, 2015). However, most of the research has been based on developing the most cost effective and efficient components and by extension systems. With the drop in the cost of PV arrays and the support by governments of green energy, it becomes paramount to design standalone systems that would be cost competitive with the conventional diesel-powered systems still in use in some remote areas.

In this quest, most researchers have been using techniques to optimize the different components separately. With these, the impact of the changing weather conditions on the performance of the PV panels and the irrigation water requirement is not considered. Campana et al.

(Campana, Li, and Yan, 2013), developed a dynamic model for solar water pumping used in grassland restoration and reducing effects of desertification in water in China. The integrated approach however considered reversing grassland irrigation with alfalfa. There is a need for research based on the systemic approach of designing SAPV water pumping carried out on irrigating food crops and especially in Kenyan hot arid lands with 1.8% of the land under irrigation. The hourly simulation of the whole system for the growing period is meant to ensure that it fulfils the demand throughout the growing season. The climatic factors that affect the performance of the system are taken into account to bring it as close as possible to the functioning of the real installed system.

1.1.2 Importance of the research

The study will come to give information to the investment companies and research institutions that are involved in climate mitigation in arid regions in fronting the use of solar PV for the green revolution. It will give them an insight into the profitability and possible ways of optimizing the system to achieve overall system reliability for installation companies and farmers.

The research also helps farmers in climatic conditions categorized as semi-arid to hot arid agro-ecological zones on the technical feasibility and economic benefits of using the SPIS to increase their farm productivities. This forms a platform to disseminate the systems as it encourages acceptability due to reduced system cost and reliability. The research also comes to inform governments and NGOs involved in food and poverty alleviation strategies in these rural areas on the techno-economic feasibility of deploying SPIS in arid areas. These are the areas that are affected a lot during times of famine in developing countries.

1.1.3 Research Questions

i. How does water demand by maize and power productivity of PV cells from weather changes during a planting season affect SPIS sizing?
ii. How does dynamic modelling help in optimization of SPIS?
iii. Is a standalone PV water pumping system technically and economically feasible for irrigation in hot arid climates as compared to diesel water pumps?

1.1.4 Main objective

The aim of this research is therefore to develop a dynamic model for a standalone water pumping system to irrigate maize in a hot arid remote area in Kenya using a water saving technology

1.1.4.1 Specific Objectives

1. To design and size a standalone PV water pumping system to be used to irrigate maize in a hot arid area in Kenya.
2. To develop an integrated dynamic simulation of the whole system
3. To examine the effect of environmental variability on the effectiveness in optimal design of standalone solar water pumping
4. To perform a Techno-economic comparison of Solar Water pumping and diesel water pumping for irrigation in hot arid climates.

1.1.5 Delimitation

The study incorporated the effect of module performance with respect to irradiation and temperature. However, the cooling effect of wind on PV array performance was not considered. This might have bolstered the performance of the arrays. As studied by Gokmen et. al (Gokmen et al., 2016), significant wind speeds can have a significant effect. It is presumed that the wind speeds are low.

Storage is key in catering up for the uncertainties of cloud cover presence. In this study, however, a directly coupled solar water pumping system is designed and simulated. It is assumed that the weather data provided by the MERRA-2 model caters for cloud cover and reduces irradiation values respectively and that the water requirement during the night is minimal compared to day requirements.

1.1.6 Thesis outline

Chapter One-Introduction: Introduces the topic giving the background information, identifying the knowledge gaps and setting objectives and the scope of the thesis

Chapter Two-Literature Review: Gives the food shortage and irrigation status in Kenya, water saving irrigation strategies and studies on design and optimization of stand-alone PV systems/SPIS.

Chapter Three-Methodology: Details the methodology and models used in dynamic modelling, optimal design, simulation and economic analysis.

Chapter Four-Results and Data analysis: presents the data and the results deduced from their analysis.

Chapter Five-Discussion, Conclusion and Recommendations: this chapter presents the discussion pints of the master thesis results. It also gives the findings arrived at with the limitations encountered. The section also proposes recommendations for further research

CHAPTER TWO: LITTERATURE REVIEW

2.1 BACKGROUND

This chapter provides an analysis on the previously conducted research in trying to develop a reliable and cost effective standalone PV system for pumping applications in remote areas. It serves to provide the knowledge on methods that have been fronted by researches to design, size and optimize SAPV systems to provide reliable and cost-effective systems. It also gives the status of irrigation and SPIS as it relates to Kenya.

2.1.1 Food security and Irrigation potential in Kenya

Various countries faced famine at the beginning of 2017. The most affected countries were Yemen, Nigeria, South Sudan, Kenya, and Somalia. An estimated 3 million people were facing starvation and hunger in Kenya caused by the drought that had ravished the country (Aljazeera, 2017). The long and short rains were not regular and therefore the harvests were low the previous crop cycle. The situation resulted in the government subsidizing maize imports as inflation and market challenges had pushed the cost of maize flour to prices not afforded by many households (FAO, 2017). An average of 46% of Kenyans live below the poverty line (under a dollar a day). This necessitates programs to alleviate food security in the future(SolarAid, 2014).

The biggest portion of Kenya's land (80%) is categorized as arid and semi-arid. Of the total land, the country has managed to put only 1.8% under irrigation compared to the sub-Saharan African average of 4%. Although the government has been showing a strong emphasis on agriculture by the provision of extension services and subsidizing inputs, increased investment in irrigation is essential to open up the drylands (Karina & Mwaniki, 2011).

The government has undertaken initiatives under the economic stimulus program to develop large irrigation schemes. Galana-Kulalu irrigation scheme is the biggest with USD 42 million having been allocated (NIB, 2016a). However, lessons have been learnt on the collapse of Bura and Holla irrigation schemes which were using diesel pumps to abstract water. They became too costly as fuel and maintenance costs soared with time and have been rehabilitated by constructing gravity canals (Alushula, 2017). For small scale irrigation farmers, they have slowly started adopting Solar PV to power their irrigation pumps (Reuters, 2016).

2.1.2 Water Saving Technologies

Water use is critical in arid and semi-arid areas where water scarcity is rampant. It is also from the energy perspective that water saving technologies have been adopted. The performance of irrigation systems is expressed as efficiency (Pereira, Cordery, & Iacovides, 2012). According to Irmak et al. (Irmak, Odhiambo, Kranz, & Eisenhauer, 2011), the performance can be evaluated using: application efficiency, irrigation efficiency, soil water storage efficiency and water conveyance efficiency. In choosing an irrigation system, water conveyance efficiency, application efficiency, and irrigation efficiency are considered.

The water conveyance efficiency refers to the portion of water reaching the field. It is expressed as

$$\eta_{CO} = \frac{V_t}{V_s} \times 100 \qquad (1)$$

Where V_t and V_s represent the volumes of water transmitted to the field and amounts of water supplied respectively. The difference is attributed to leakages, diversions (illegal) and evaporation.

Water application efficiency is the amount of water stored in the crop rootzone to the amount of water reaching the field

$$\eta_{a} = \frac{V_r}{V_t} \times 100 \qquad (2)$$

Where V_r and V_t are the amounts of water stored in the rootzone and the amount of water transmitted to the field respectively. Losses contributing to this efficiency is from evaporation and wind drift.

Water may be used for other purposes including cooling, leaching salts and preparing the seedbed. Irrigation efficiency therefore to the amount of water used for the crop and the total amount of water used.

$$\eta_{i} = \frac{V_b}{V_t} \times 100 \qquad (3)$$

Where V_b and V_t represent beneficial water used and delivered water respectively.

The overall irrigation efficiency is therefore expressed as a product of application and conveyance efficiencies. This is used to assess which irrigation technology saves more water. Comparing irrigation efficiencies of systems that can be applied with solar PV, micro-irrigation especially drip systems exhibit higher efficiencies (Levidow et al., 2014).

$$\eta_{O}=\eta_{a} \times \eta_{CO} \quad (4)$$

2.1.3 Standalone Solar Powered Water Pumping Systems for Irrigation

The main systems being used currently to power irrigation is electrical grid connected and diesel-powered water pumps. Using Bangladesh as an example, the country uses 15% of total generation in pumping while India's irrigation systems employ 23% of the grid and nearly 15% of diesel (FAO, 2015). The pressure on the national grid and the unsustainability in the use of conventional power sources have pushed them in pursuit of more viable green options in the form of biomass and Solar PV systems.

With the predicted exhaustion of world fossil fuels and the externalities associated with the use of these resources, the countries have turned to renewable energy resources to power the future (FAO, 2015; Twidell & Weir, n.d.). No wonder there is continued support from governments and financial institutions to invest in green projects. Apart from Geothermal, hydropower and nuclear power which have high capacity factors, investment on the other green energy sources anchors on reliability and cost. This has been somehow compensated by policies that support feed in tariffs and net metering to improve stability.

Access to electricity is still low in Africa but not for North Africa and South Africa. In Kenya, the national electrification rate was a mere 23%. However, investment by the government, especially in Geothermal resource and power distribution, through set up departments including Rural Electrification Authority (REA) has seen this rise to 56% in 2016. Rural electrification still remains lower than the national average, however. Electricity demand has been growing by 5-8% (Hille & Franz, 2011). The use of off-grid systems and mini-grids has been deployed but very remote areas haven't been overly reached, although, through the government's initiative like the last mile connectivity, it is expected to reach 70% by 2020. Remote areas still rely on diesel engines, standalone PV systems, and small home systems as a source of their power for lighting and agricultural applications but biomass, kerosene and LPG cylinder dominate the cooking functions.

The prices of PV panels and accompanying balance of systems have reduced by nearly 62% in the period from 2009 to 2015 with a further expectation of 59% reduction by 2025 (IRENA, 2016b).

It is therefore paramount that these systems have to be designed in a manner that they provide reliable power while remaining economically viable. This ensures more acceptability of these energy sources (Posadillo & Luque, 2008). In other instances, a combination of two or more systems has been used as irrigation systems. Solar has a strong correlation between the water requirement and available solar radiation (Ghoneim, 2006) together with low maintenance and environmental friendliness. Kenya is party to the Paris Agreement and has set reducing carbon emissions through its Intended National Determined Contribution (INDC) (Michaelowa, Kohler, Friedmann, Drasfield, & Tkacik, 2016)

The use of solar water pumping for irrigation has gained momentum. Countries in the recent past have embarked on ambitious plans to establish programmes to increase their dissemination. Its popularity has been mostly attributed to the dipping of the cost of PV modules and cognizance of the benefits of the systems. For instance, Bangladesh, India, and Morocco set to deploy 100,000 solar irrigation systems by 2025, 2022 and 2020 respectively while the Malawi is expected to set up a 500-hectare farm financed by the African Development Bank (IRENA, 2016a).

The civil conflicts in Syria have caused unreliability in electricity supply. This experience has led to farmers and homesteads alike using solar water pumping systems to supply drinking water and IWR for drinking and irrigation respectively. The unreliability of distribution is also a factor in Africa whose irrigated land is less than 6% compared to the world average is 20%. The potential has introduced social enterprises as well as government initiatives to improve this (Wheeldon, 2016).

Since 2013, solar irrigation in Kenya has expanded tremendously with the entry of various companies into the scene. SunCulture and FuturePump among other small companies have introduced packaged products and often combined with some financing programmes to enable smallholder farmers to overcome the hustle of high initial costs. The companies operate almost on similar dissemination models thanks to the infiltration of mobile money transfer in Kenya. The farmer pays a down payment with the remaining paid in instalments via mobile money transfer. It has helped farmers overcome the upfront costs on capital costs while also accessing markets arranged by the companies (Wheeldon, 2016).

2.1.3.1 Solar Photovoltaic Water Pumping Configurations

A solar water pumping system consists of five basic components: a solar PV array to convert irradiance to useable electricity, a power conditioning system (charge controller and inverters), a motor to drive the pump, a pump to deliver the water and an energy storage. Energy storage can be a hydraulic storage (tank) or an electric storage (battery). A wiring, piping and mounting system is also part of the installation and can be either tracking or fixed.

Various configurations are used with various components chosen depending on various influencing factors.

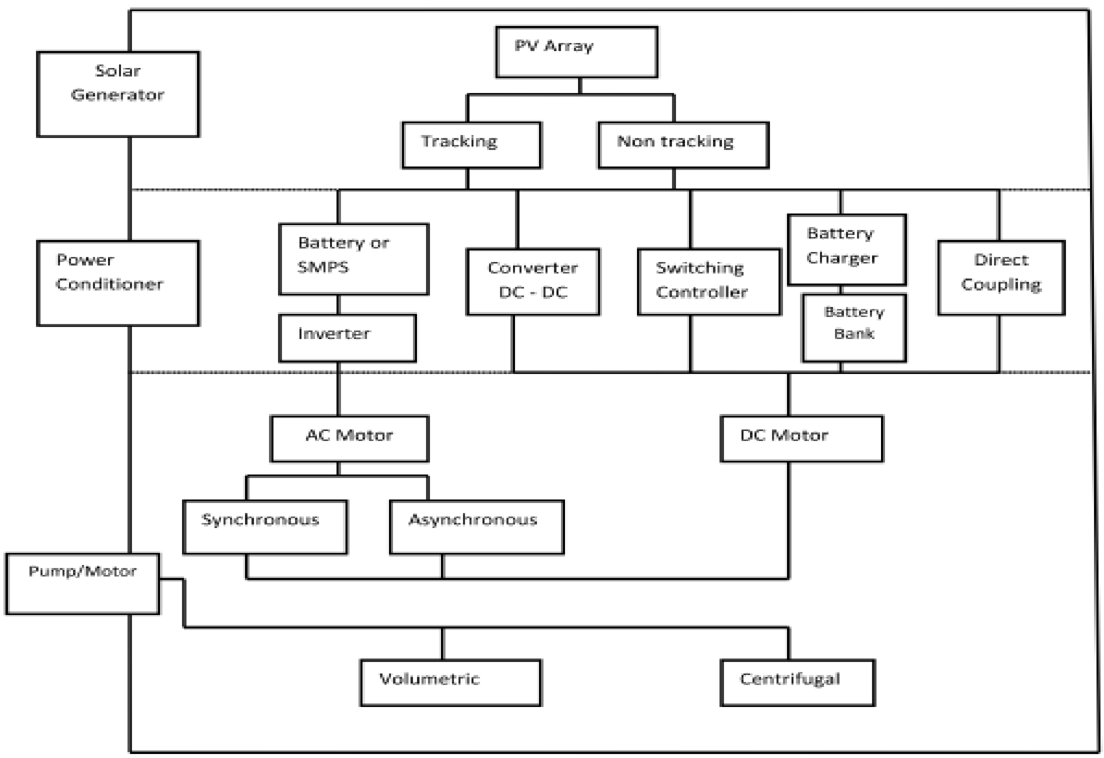

Figure 1: Configurations for SPVWPS (Shrestha, Kumar Jha, and Karki, 2014)

According to Chand & Kalamkar (2016), the configurations can be categorized based on energy storage, type of input power, type of pump and mounting.

Energy Storage

This categorization is dependent on how the generated electric power is stored, with no storage or with storage. Battery coupled solar pumping system incorporate a battery and a charge regulator. When the battery is online the electricity generated passes via the battery and the battery powers the pump. The charge controller functions to prevent the battery from overcharging or being completely drained. A set up to have the power to directly power the pump when the battery is full is also possible. The batter functions to provide the power during days of autonomy and at night. Batteries are however expensive, reduce system efficiency and limit operating voltage.

In directly coupled systems, the power generated by the PV array is used directly by the pump. The water pumped and efficiency is also dependent on the amount of solar insolation incident n the PV array. It is paramount therefore to do proper sizing of the system to match the load. Hydraulic water storage (water tank) may be used to cater for cloudy days and night when less or no power is generated by the PV array.

Power used

Solar PV modules produce DC current. However, depending on the type of motor chosen, they can be driven by AC or DC current. If AC current is required, the output current from the PV array has to be conditioned to produce AC current by use of an inverter. DC pumps are either DC motor utilizing brushes or brushless permanent magnet DC motored pumps (Chand and Kalamkar, 2016). Frequent maintenance of DC motors with brushes limits their use. Brushless DC motored pumps exhibit higher cost, but are boosted by their higher efficiencies and low maintenance (Pullenkav, 2013).

AC water pumps utilize an inverter to obtain AC current from the generated DC current. The pumps are generally cheaper and readily available. However, their use in standalone PV pumping has been inhibited by their high starting current, low efficiency and increased the additional cost of conditioning inverters (Shrestha et al., 2014).

Pump type installation

The pump’ installation depends on its position in relation to the suction and delivery points respectively. Chandel, Nagaraju Naik, and Chandel (2015) classify solar pumps as deep-well pumps (submersible and floating) and surface water pumps. The respective height of suction and delivery varies with the water level in floating pumps. Surface pumps are used for shallow water levels such as surface water and shallow wells while submersible pumps are normally used for underground water pumping. Cavitation, extreme weather conditions and loss of priming are some of the inadequacies of surface pumps. They can be further classified as dynamic or positive displacement pumps as a factor of their mode of operation. Consideration of irrigation demand, delivery height, and water quality characteristics influence the selection of solar water pumps for irrigation purposes.

PV array mounting

The mounting of PV arrays is a factor of the tilt angle to obtain optimum insolation. It is either fixed angle mounting, single axis tracking or double axis tracking. Although the cost of the mounting system is low, fixed angle mounting results in lower amount of insolation received by the PV array and necessitates additional PV size to cater for this.

Axis tracking has an MPPT tracker that functions to follow the direction of the sun so as to be normal on the PV array thereby receiving maximum insolation. Single axis tracking follows the direction of the sun according to the hour of the day. Double axis tracking, on the other hand, is able to track the position of the sun during the day and according to seasons and results in additional insolation on the solar panels of 30-40% elevating the efficiency of the system by up to 20% (Campana, 2015; Chandel et al., 2015)

Solar energy is stochastic in nature, affected by the variation in the weather conditions and the changing position of the sun in relation to the solar panel. As such, sometimes it doesn't meet the demand when called upon as the load and the supply do not peak concurrently. It is with this in mind that studies have been conducted that recommend hybridization of the systems and have a battery backup that acts as an auxiliary source. In essence, the battery size becomes small with these configurations.

2.1.3.2 PV array modelling

The PV module acts as the electricity generator, turning solar radiation into electricity. Many studies have proposed models to predict the power generated as well as the current voltage characteristics of the PV array, and their complexity differing.

Dongue, Njomo, & Ebengai, (2013) postulated an improved single diode non-linear five-point model that characterizes the PV array performance. They argue that the simplified models used in other simulation tools are inaccurate and either understate or overstate the economic returns. Their validation using experimental data from three types of PV cells showed fewer errors than other proposed models due to their choice to have the parameters vary with both the irradiance and temperature. High errors were however discernible near the MPP due to the impact of series resistance in shaping MPP point.

Zhou, Yang, & Fang, (2007) proposed a novel model that is based on the calculation of five parameters: α, η, γ, β, R_S based on the manufacturer's parameter charts and sheets. They then estimated the performance of the modules under clear skies and on a clear sunny day. The measured data showed a strong statistical correlation with coefficients of determinations R^2 returning values of 0.98 and 0.96 on clear sunny and cloudy days respectively. They attributed the lower value on cloudy days to the fast-changing conditions from the movement of clouds. This is also supported in Soto, Klein, and Beckman (2006) with use of experimental data from National Institute of Standards and Technology and Sandia National Laboratories for hourly value determination of the solar irradiances recorded for a period of 12 years (Fanney et al., 2006).

The use of peak solar hours (PSH) has been used by Firmanda, Riza nd Gilani, (2014) in determining the power output used in supplying a residential house in Malaysia. An hourly simulation is done using TRNSYS to evaluate the outcome of the sizing procedure resulting in a reduced figure of the factor used to measure reliability, LPSP, insinuating that the design met the demand expectations of the house.

The above studies on power modelling of the PV array either had a constant temperature or temperature incorporated as the factor of the operational efficiency of the PV module. Hellman et al. (Hellman, Koivisto, & Lehtonen, 2014) used a regression model for hourly radiation by fitting calculated and theoretical using solar radiation model from Rigollier et al. (2009) and using Linke Turbidity data. Linke Turbidity is used to mean the threshold of clearness and humidity in the atmosphere that would reduce the intensity of radiation reaching the surface of the earth (Abdul-wahid and Judh, 2009). It showed good correlation with the measured data, though mostly on horizontal surfaces but Hellman et. al finding expressed delimitations of high angles of incidence and the factor of the cooling effect of wind on the PV modules.

2.1.3.3 Inverter Modelling

To model an inverter, the configuration of the system varies. An on-grid inverter for power systems that supply power to the grid and directly to appliances, an off-grid inverter or centralized inverters that may also incorporate charge regulators moderating power to the storage while also power is being drawn for powering the load. The model of the inverter depends on the power from the module.

2.1.3.4 Sizing of standalone Photovoltaic system

Sizing SAPV system involves developing a system that will meet the load with a predefined acceptable tolerance level. In order to start designing and optimizing the PV system that fits a certain area of interest, the criteria for appraising it is paramount. In order to supply power for irrigation pumping in this location, the most feasible power source is evaluated based on these criteria (Khatib, 2010; Khatib, Ibrahim, and Mohamed, 2016). They are represented by various interest groups in the form of stakeholders ranging from investors, communities, consumers and governments among others (Hosseinin, Ghaderi and Shakouri, 2012). All these views are subjected to a decision mechanism to obtain the most feasible solution.

Many solutions have been adopted in a bid to include more criteria and ease decision making. Garni, Kassem, Awasthi, Komljenovic and Al-haddad (2016) used multicriteria decision mechanism of analytical hierarchy process (AHP) to assess the viable options for renewable energy resources for providing power to Saudi Arabia in a mid-term scenario. Brand & Missauoui, (2014) used the TOPSIS approach to evaluate Tunisia's energy generation mix. Various other methods for evaluating projects have been used in ranking energy projects by researchers including Goletsis, Psarras, and Samouildis, (2003). Đurin & Baić, (2016) used PROMETHEE to determine the optimal variant in sizing solar power irrigation system in Algeria.

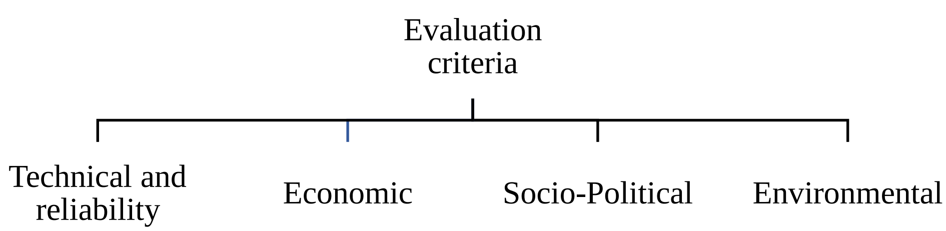

Figure 2: Criteria for assessing energy projects

2.1.3.5 Technical and Reliability criteria

The methods used to assess the reliability of energy from intermittent generation sources can be grouped according to (Hee Yau, 2006):

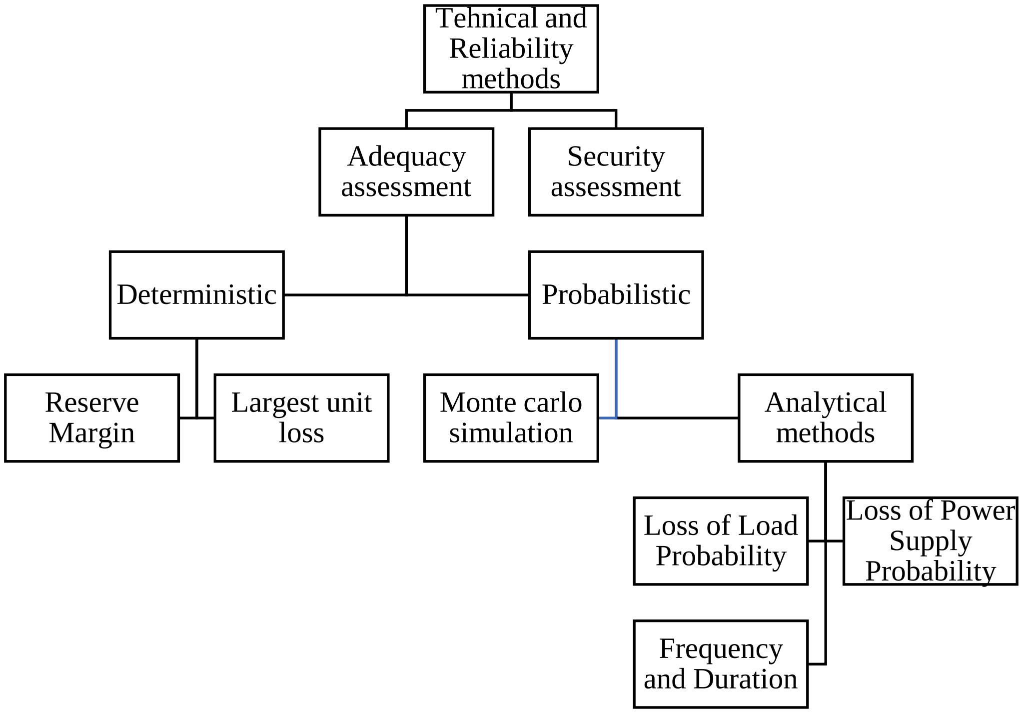

Figure 3: Technical and Reliability Criteria

The review will focus on the most commonly used criteria used in providing reliability to power systems.

Loss of Power Supply Probability (LPSP) represents the chance that power generated by the system including a storage and an auxiliary energy source e.g. in hybrids, cannot give power to the load when called upon i.e. during demand (Abouzahr and Ramakumar, 1991). It has been the most used criteria in sizing especially in hybrid systems (Ofry and Braunstein, 1983). It can be expressed as loss of power supply (LPS) during a specific duration as a fraction of cumulative load demand (LD) over the same duration (Khatib et al., 2016)

$$LPSP = \frac{\sum_{t=1}^{N} LPS(t)}{\sum_{t=1}^{N} LD(t)} \qquad (5)$$

With LPS(t) expressed as a deficit of Load demand against energy generated at a specific time which returns a value when the load is not being met and zero when demand equals energy generated.

Loss of Load Probability (LOLP) measures the futuristic value of the duration that the load on the system would exceed the generation capacity of the system (Hee Yau, 2006). It is mathematically derived as

$$LOLP = \frac{\sum_t^T DE(t)}{\sum_t^T P_{load}(t)\Delta t} \qquad (6)$$

DE(t) represents the shortfall of the system to provide energy to the load during a certain temporal space, $P_{load}(t)$ represents the demand during the same time space while Δt represents joint time under consideration of load and supply.

Autonomy Level (AL) is a value which gives the percentage duration of operation in which there was no loss of load. It is therefore given by (Celik, 2003):

$$AL=1-\frac{H_{LOL}}{H_{OT}} \qquad (7)$$

where H_{LOL} and H_{OT} represent the duration of loss of load and operation time (hours) respectively.

Total energy loss (TEL) represents the excess power produced over the required power by a given generation system. A pre-determined value is set over which the total quantity generated should not exceed in a set time period, usually annual (Alsayed, Cacciato, Scarcella, & Scelba, 2013). It is expressed as:

$$TEL = \sum_{t=1}^T E_g(t) - LD(t) \qquad (8)$$

This could be treated as waste energy generated and could involve additional capital, operation, and maintenance cost of equipment. This may bring additional cost, especially where there is no place to damp the excess power in the form of extra utilities to supply, in places where there are no policies for feed in tariffs and net metering mechanisms or very remote locations.

2.1.3.6 Economic criteria

Life Cycle Cost (LCC) represents the cumulative summation of all the costs incurred in generating energy for the project over its lifetime. It is normally discounted to get a constant value in present terms. It includes initial capital costs, installation costs, fuel costs, operation costs and costs for mitigating externalities such as pollution (Jakhrani, Othman, Rigit, Samo, and Kamboh, 2012).

$$LCC = (ICC + IC + O\&MC + RC + PMC) - SV \qquad (9)$$

Where ICC is initial capital cost; IC, installation cost; $O\&MC$, operation and maintenance cost, RC, replacement cost; PMC, pollution mitigation cost and SV the salvage value of the system equipment.

LCOE is used in comparing the price of energy from various sources. It is defined as the annualized cost of the system as a ratio of the annual electricity that can be obtained from it.

CRF is expressed as

$$CRF = \frac{r(1+r)^n}{(1+r)^n - 1} \quad (10)$$

with r and n representing the discounting rate and the lifetime of the system.

Payback time represents the amount of time it takes for the project to return the capital invested in it. Simple payback time is given by (Twidell & Weir, 2000):

$$PBT = \frac{ICC}{CF} \quad (11)$$

This method assumes that the cashflows are constant during the entire period and doesn't take into account the inflationary or discounting rate.

The net present value (NPV) is used to assess the profitability or economic viability of a project. It is defined as the net present value of cashflows subtracted by the net present value of incurred costs during the lifetime of the project. It is defined according to the equation:

$$NPV = \sum_i^n \frac{(CF - (O\&MC + RC + PMC))_i}{(1+r)^i} - ICC \quad (12)$$

2.1.4 Sizing methods for stand-alone systems

The normal procedure for developing a standalone PV energy system includes first locating the site where the project is to be undertaken. Having obtained the metrological data of the area, the size of the various system components is determined while considering the load it is intended to supply power to. System size optimization is meant to make the energy system operate at the best possible situation (Khatib, 2010). Several methods have been fronted for sizing stand-alone energy systems which by extension are used to size SAPV systems. Others are mature while others are still under development and new e.g. artificial intelligence.

The optimization methodologies can be categorized according to:

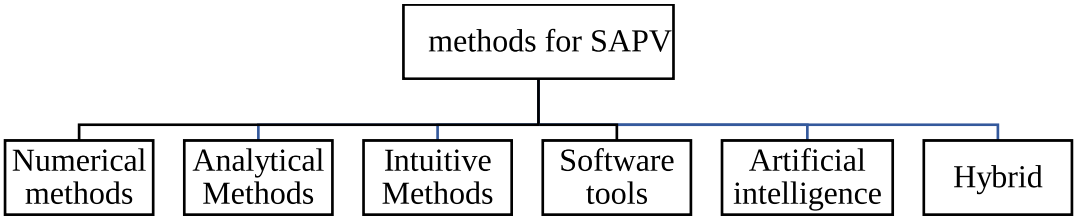

Figure 4: Categorizing Methods for optimal sizing of SAPV

2.1.4.1 Intuitive methods

The method uses a simplified calculation taking the system as a static system and assuming non-stochastic nature of irradiation. The different subsystems are taken as isolated units. A factor to cater for safety is used during the design based on intuition i.e. past experience with designing in the area. According to Sidrch-de-Cardona and Lopez, (1998), this can use the worst month scenario to size the system. The rationale is that since it can serve during the worst month, it can work during the other months. In Khatib, Mohamed and Sopian, (2013) the sizing equations are described as:

$$P_{pv} = \frac{E_L}{\eta_s \eta_{inv} PSH} S_f \quad (13)$$

where $E_L, \eta_s, \eta_{inv}, PSH, S_f$ represent the daily load demand, system efficiency, inverter efficiency, peak solar hours and safety factor respectively.

The battery capacity is given by

$$C_B = \frac{E_L N_D}{V_B DOD \eta_B} \quad (14)$$

Where C_B, N_D, V_B,DOD an d η_B represent the battery capacity (Wh), number of days of autonomy, battery voltage, depth of discharge and battery efficiency respectively.

Bhuiyan and Asgar (2003) designed by taking the month with the lowest insolation and try to find the best array size, tilt angle, and battery storage. The optimum sizes to provide power to a residence in Dhaka was found for different seasons and hence necessitated tilting the solar array in accordance with seasonal variation. This provides structural challenges in installation and more often lead to oversized/undersized systems.

Ahmad (2002) used the equations proposed by khatib et. al (Khatib et al., 2013) in sizing a PV system for powering a house in Egypt that includes an underground pumping system. Although a correction factor for temperature is used to take consideration of the loss of efficiency from temperature deviation, the charge regulator which is chosen is the one that will make the battery last longer. The inverter safety factor is also arbitrarily fixed at 20%. The system was however found to be competitive from the economic standpoint.

Kaushika and Rai, (2006) developed an expert aid system using 14 stations in India by combining location as well as PV cell characteristics to form a parameter based on the geographical coordinates. They propose that the parameter can be used for general sizing in the Indian region.

Chel, Tiwari, and Chandra, (2009) did an integrated optimum sized PV energy system a building in India. They used peak sunshine hours and average daily energy consumption. The components were optimally sized based on LCC and LCOE and capital costs.

2.1.4.2 Analytical Methods

Analytical methods for SAPV systems develop mathematical relationships of the different systems components and express them as a function of reliability so as to evaluate the viability of the energy system. The performance of the systems based on single or multiple performance indices to assess different system sizes and configurations. It includes finding coefficients which have a drawback that they are specific to a certain locality and have a complexity in their determination. However, the methods are easy to use (Chel et al., 2009; Khatib et al., 2016).

Zanesco et al. (2006) evaluated an analytical method by finding battery storage capacity and solar array area that will fulfil the demand under the solar irradiance with an acceptable LOLP. They determine the isoreliability curves expressed in terms of clearness indices and latitudes. They then developed and installed SAPV for Porto Alegre-RS-Brazil using the method with results showing that the system supplied the load as predicted.

According to Gordon (1987), analytical optimization methods are based on the random characteristics of processes. He based his experiments an assumption that the climate data is based on a Markovian (influenced by recent historic processes) and developed a one-step model using input irradiances as net input values resulting from this theory. He used a correlation coefficient to represent the probability distribution of insolation.

2.1.4.3 Numerical Methods

With the advancement in recording equipment and sensitivity and increasing number of stations, data for many locations with a small-time scale can now be obtained with more ease. Predictive statistical models also can provide data to small temporal units such as a minute. Numerical methods use instantaneous energy balances so simulated the whole system for the period under consideration. It leads to more accurate refined results, however daily or hourly data for a long duration is required, which may not be available for remote locations (Sidrch-de-Cardona & Lopez, 1998).

Kazem, Khatib, and Sopian (2013) developed a numerical method for sizing a PV/battery for providing electricity to a house in Sohar, Oman, by using MATLAB simulation of the demand and the hourly climatic data for the location. They optimized the tilt angle, battery capacity, and PV array by basing it on the LCOE which they optimized to 0.196 USD/kWh

In developing an optimal configuration, various peak power generated by the PV array and optimum battery capacity result. While selecting an optimum configuration for a site in Algeria, Arab et al. (Arab, Driss, Amimeur, & Lorenzo, 1995) used total system cost based on the reliability factor of LOLP. While using the clearness index to depict various climatic zones in the 12 sites he used, he did a simulation considering 10 years.

2.1.4.4 Artificial Intelligence

Artificial intelligence is the latest techniques to be employed in sizing of RES. They are suited for use in optimal sizing of standalone energy systems in remote areas where the climatic data may be unavailable and the stochastic nature of the solar insolation. They are more versatile and have the potential to provide improved, expeditious and pragmatic solutions than conventional methods, however, they need high level computation (Kalogirou & Arzu, 2010). The techniques can be grouped as forecasting algorithms and seeking algorithms.

The methods have gained importance in predicting the performance of SAPV systems. Haddad et al. used the ANNs-based model to predict the water flow rate of a PVWPS installed in Medinah, Saudi Arabia (Haddad, Benghanem, Mellit, & Daffallah, 2015). This uses the data collected from a PVWPS installed in the area. The model developed would give precise hourly flow rates with inputs of hourly ambient air temperature and solar radiation.

A Mellit, (2006;2008) used ANFIS to develop an algorithm that is used to predict the optimal parameters of sizing SAPV systems in Algeria. It used a numerical model of 200 geographical sites in the country. The model was validated from already sized parameters and showed a strong correlation. He proposed the model could be used for other locations in the country with only the geographical coordinates being required. In (A Mellit, 2008), he has incorporated GA to determine isoreliability curves. GA follows the system of evolution to search for a viable solution with mutation, crossover, and selection of parents and offspring to within a given search space. It is recursive and hence stops when a global optimum is reached.

Other intelligence based techniques include Ant Colony, Particle Swarm Optimization, Evolutionary programming, Artificial Bee Algorithm, Simulated annealing, Biogeography based optimization

Ganesan, Vasabt, and Elamvazuthi (2017) used type II Fuzzy modelling in multi-objective optimization of SPIS. In combination with bacteria foraging algorithm, they catered for environmental uncertainties. This was a case of finding an optimum solution in presence of noisy environmental parameters like temperature and solar radiation.

Ouachani, Rabhi, Yahyaoui, Tidhaf, and Tadeo (2017) used TOR and fuzzy logic algorithms in optimizing water pumping systems that utilize wind and solar energy. Their aim was to compare the method that would preserve more charge with a higher reliability of the system. Both algorithms yielded similar results although but for some minor differences. The fuzzy logic utilized all the wind energy with a higher state of charge of the batteries.

(Glasnovic and Margeta (2007a) used a dynamic hybrid programming model to optimize a solar pumping irrigation system. The model was verified for a place in Croatia and showed a strong correlation with the measurements with the installed system. It also exhibited smaller deviations than other common sizing methods.

2.1.4.5 Software tools

These are computer tools which have inbuilt methods for sizing and optimization. They have the advantage of simplicity and refined outputs. The common software for sizing, simulation, and optimization software are reviewed.

According to Turcotte, Ross, Sheriff, Blvd and Tel (2001), the software can be grouped into: appraisal software utilized for general sizing and economic viability, sizing software for optimal sizing of the system and energy balancing, simulation tools that allow manipulation of the system details to achieve a certain output, and open architecture software that the interaction algorithms can be changed.

RETScreen is an appraisal tool developed by Ministry of Natural Resources, Canada. It is intended for decision makers to assess the technical and financial parameters of projects ("RETScreen | Natural Resources Canada," 2017). Its application ranges from PV systems to water pumping systems using a NASA meteorological database. It has an excel display but it operates on a visual basic platform. It has an advantage of simplicity but its use in accurate calculation is inhibited by inability to take consideration of PV array performance dependence on temperature

Rezae and Gholamian (2013), conducted a technical and financial analysis of an irrigation farm in Gorgan, Iran, using RETScreen. From the study, they concluded that the use of solar water pumping system led to a reduction in the cost of production and operation. After payback time, the system is able to post significant returns with the only challenge being the capital costs.

Transient Energy Simulation program (TRNSYS) was initially developed for thermal energy system simulation by the University of Wisconsin, Colorado. Based on FOTRAN code, it has since been upgraded to include other energy resources including solar PV. Campana et al. (2013) used TRNSYS to do a dynamic modelling of solar water pumping for irrigation to be used for grassland restoration in China.

The Hybrid Optimization Model for Electric Renewables (HOMER) was developed by National Renewable Energy Laboratory (NREL). Using C++ platform, the tool is used for appraisal, configuration comparison, and sensitivity analysis. Kazem et al. (2016) used HOMER in designing a solar water pumping for Oman and subsequent analysis indicated the solar water pumping system had a capacity factor of 23% and LCOE of 0.306 USD/kWh. Measurements from the system were used to validate the system which proved to meet peak energy loads.

This is an improved Hybrid Optimization by Genetic Algorithm (iHOGA) developed by the University of Zaragoza runs on a C++ platform. It incorporated various renewable energy sources and does optimization by Genetic Algorithm. It has been upgraded to accommodate the life cycle emissions and revenue generation from sale of energy to the grid.

PVSYST is used in system sizing of SAPV systems based on LOLP factor in optimization of the system components and orientation. It uses monthly averages as well as hourly climatic data. Raturi (2011), used PVSYST to conduct a feasibility of using solar water pumping for a rural village in the Fiji Islands

CHAPTER THREE: METHODOLOGY

3.1 MODEL DEVELOPMENT

In order to carry out the research, the tasks in this section will be divided into five parts: the site characteristics of the area, the assessment of the available solar radiation potential, determination of the irrigation water requirement, system configuration sizing, dynamic modelling and simulation of the system and economic analysis.

3.1.1 Conceptual Framework

The research will be carried out as outlined in the stages in Figure 5. From the irrigation water requirements by the crops and the borehole characteristics, the hydraulic energy demand is determined. A pumping system is chosen that will meet the water requirement. Comparing the hydraulic energy demand and the amount of solar insolation, a PV array and power conditioning that will meet the requirement is determined. The hourly dynamic modelling is a continuous integrated process in which the effect of meteorological, radiation and plant growth has an effect on the performance of the system.

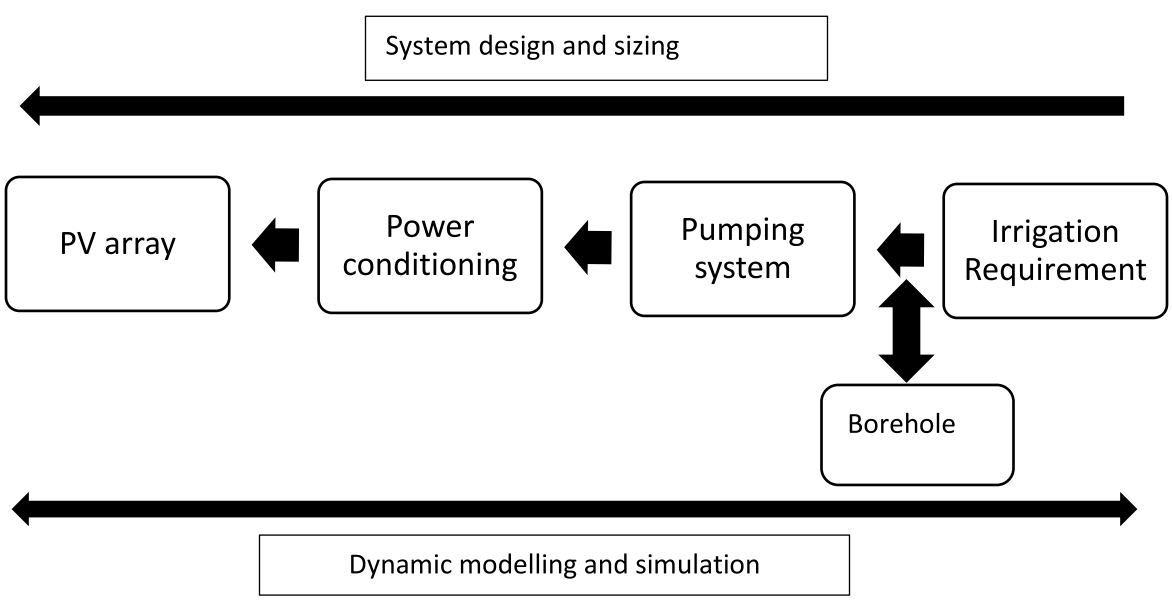

Figure 5: Conceptual Framework

3.1.2 System Description

In order to carry out the dynamic modelling of the photovoltaic irrigation system, direct coupled solar water pumping system was chosen. According to Shinde and Wandre (2016), when the solar array is directly coupled with the load, the solar pumping system is the most efficient. Thus, the intermediate phase of incorporating battery storage and or inverter is done away with in this case. The system is comprised of the solar array panels to convert the solar energy into useable electric power. The array is mounted in an angle determined by the optimisation using the PVSYST software. The power generated is connected directly to the submersible solar water pump. To provide a good compensation of voltage and current during periods of low solar insolation a power controller was installed in the interface between the solar array and the pump. For the pump chosen, the MPPT converter ins incorporated into the centrifugal pumping system. The pump chosen is a DC solar pump due to its high efficiency over AC pumps. Due to the presumption that the water needs are low during the night, no storage is used in the preliminary configuration for system design. The configuration and set up is shown in Figure 6.

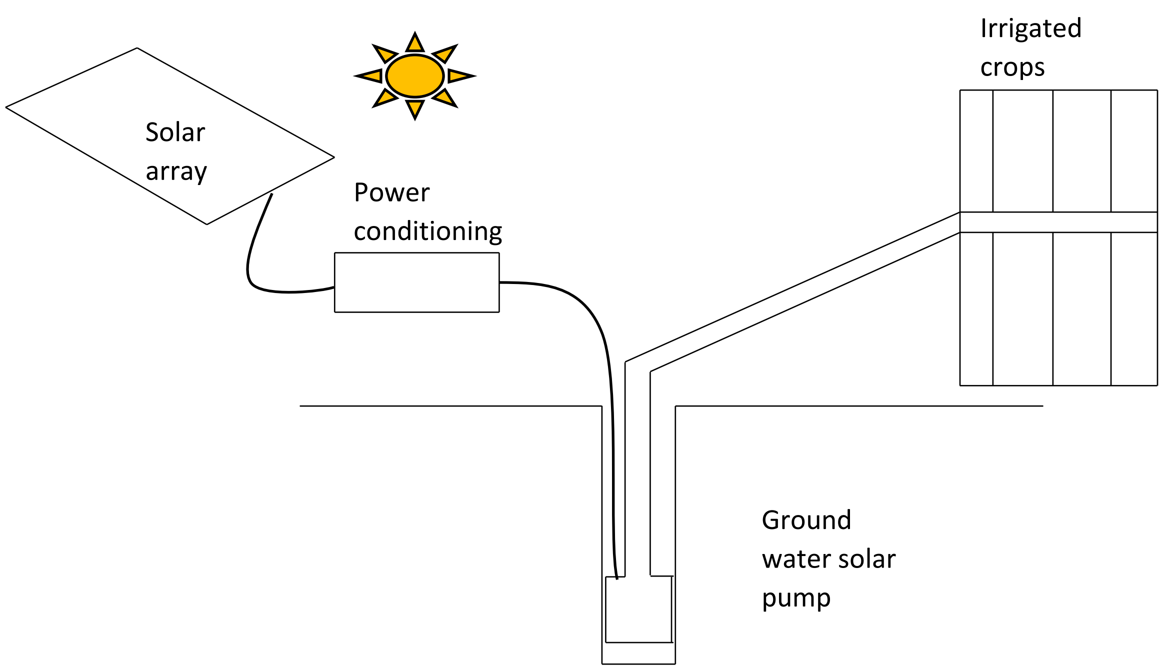

Figure 6: Solar Irrigation System Configuration

3.1.3 The study area

The study was conducted around Saretho, Garissa in the North-Eastern part of Kenya. It is an area that lies between the Daadab refugee camp and Garissa town. Daadab Refugee camp is the largest refugee camp in the World mainly inhabited by Somali refugees fleeing the instability in their country. The high population in the area has put pressure on the environmental resources, with the area suffering from food shortages and deforestation (Mude et al., 2007).

The communities in the area rely on pastoralism with some form of agro-pastoralism along the valleys of River Tana and accounting for the source of livelihood for over 88% of the population. Although the County has an irrigation potential of 32000 ha, only 3446 has been put under irrigation in floodplains and seasonal riverbeds crisscrossing the county (GoK, 2015). The Government of Kenya under the national irrigation board (NIB) has put up 7 irrigation projects in the County which rely mostly on water pans and canals for the supply of water (NIB, 2016b).

The area is categorized as semi-arid to arid under the Agricultural ecology zones with the area experiencing hot and dry climate. It receives low rainfall averaging 435 mm annually characterized as highly unreliable with the short rains being more reliable than the long rains. The long rains fall between March and May, while the short rains fall between September and December. High daily average temperatures ranging from 28-38ºC are normal (Daze, 2012).

With soils ranging from sandstone in some areas to alluvial deposits at the shore of River Tana, the area has a high potential for farming. River Tana is, however, the only permanent river in the area cutting across several counties as it discharges into the Indian Ocean. In spite of this, the area has a high potential of groundwater sources. The Merti Aquifer has fresh water especially in the southern part of the county, where Saretho is located (Mude et al., 2007).

3.1.4 Meteorological and Irradiation Data Sources

Hourly irradiance information was retrieved from Solar radiation data (SoDa) Solar Energy services for professionals based on helioclim-3. The site is maintained by Transvalor/Mines ParisTech. It provides data from 15-minute intervals to monthly intervals using the clear sky model and actual irradiation depicting actual weather conditions and covering Meteosat field of view (MINES, 2017). Hourly data wasn't available at KMD for the area.

The meteorological data also from the same site is based on the Modern-Era Retrospective analysis for Research and Applications, version 2. The system is produced from Global Earth Observing System (GEOS v5.12.4) atmospheric simulation and Grid point Statistical Interpolation (GSI). A data series for the year 2006 was used (Gelaro et al., 2017).

3.1.5 Solar irradiation in Garissa

Kenya and especially Garissa experiences high solar insolation ranging from daily insolation of 4 - 6 kWh/m^2 (IREK, 2013.). Being a hot climate, chances of reduction of PV performances are expected. Notwithstanding, up to 15% of this solar energy can be converted into useable electric power according to the solar modules chosen (Shrestha et al., 2014). Its nearness to the equator is positive for the implementation of PVWP because its value doesn't vary much with seasons.

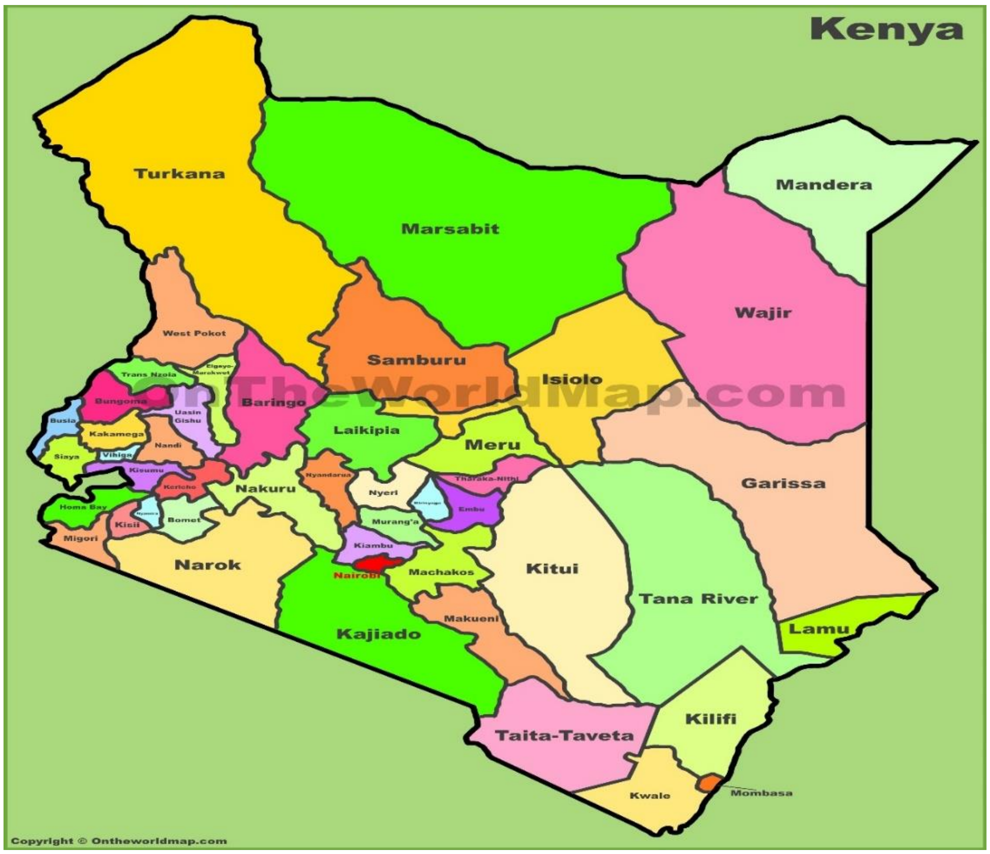

Figure 7: Location of Garissa in Kenya

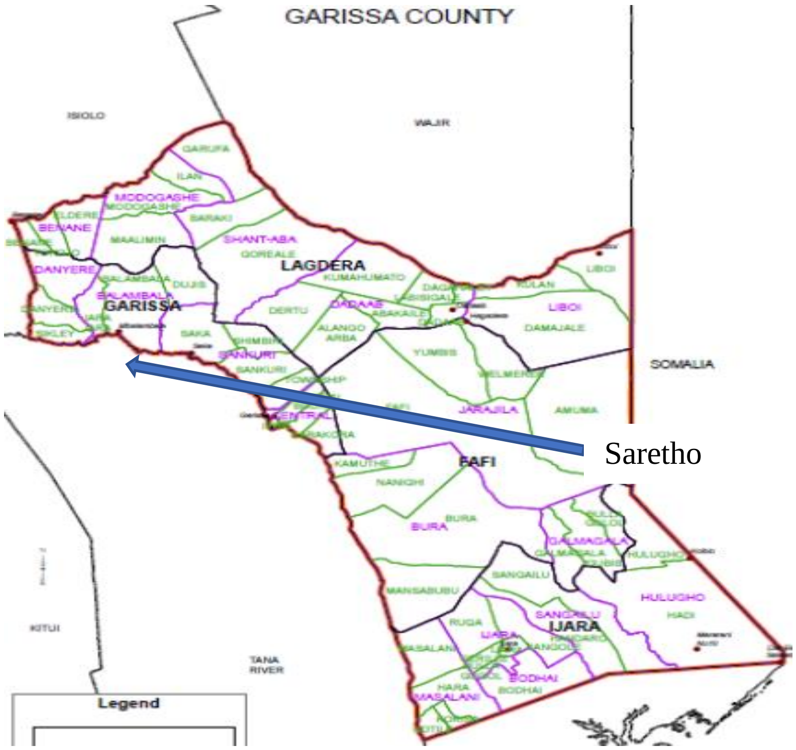

Figure 8: Garissa County

3.1.6 Irrigation water requirement

The crop chosen for the study is maize which is the staple food in Kenya and is one of the commodities that form almost every Kenyans food basket. It is also among the government's strategies to alleviate food insecurity that is currently facing the country. Maize is assumed to be under growth during the normal planting season that coincides with the long rains.

A Kenyan soil survey map was used to give a guideline on the soil characteristics in the location. To calculate the water demand by the plant and hence the irrigation water requirement, a FAO guideline (Allen, Pereira, Raes, & Smith, 1998) using the FAO Penman-Monteith equation was used to estimate the reference crop evapotranspiration with consideration of radiation, humidity, air temperature and wind speed. Based on the reference evapotranspiration and the stage of growth of the plant, cultural evapotranspiration was computed. Together with the computation for the effective precipitation received, the irrigation water requirement represents the deficit of the crop water requirement not met by the precipitation. The daily reference evapotranspiration is based on:

$$ET_0 = \frac{0.408\Delta(R_n - G) + \gamma\frac{900}{T+273}u_2(e_s - e_a)}{\Delta + \gamma(1 + 0.34u_2)} \quad (15)$$

where

ET_0 = reference evapotranspiration

Δ - Slope of the vapour pressure curve

Rn – daily net radiation on surface of crop

G- soil heat flux density

γ – the psychometric constant

T – daily mean air temperature

u_2– Wind speed

e_s – saturation vapour pressure

e_a – actual vapour pressure

The equation utilizes the normal climate data records made at 2 m above the ground surface

The meteorological data that are provided are solar radiation, daily mean temperature, wind speed and relative humidity. Therefore, supporting equations are used to ensure the reference evapotranspiration is dependent on these parameters.

Atmospheric pressure, $P = 101.3(\frac{293-0.0065Z}{293})^{5.26}$ where Z is the height above sea level and P is the atmospheric pressure

The psychometric constant $\gamma = \frac{C_\rho P}{\varepsilon\lambda}$=0.000665P where λ is the latent heat of vaporization and $C_\rho$is specific heat capacity while ε is the ratio of molecular weight of water vapour and dry air (Allen et al., 1998).

Saturation vapour pressure, $e_S = 0.6108\exp(\frac{17.269T}{237.3+T})$ and actual vapour pressure, $e_a = \frac{e_S RH}{100}$

Slope of vapour pressure curve, $\Delta= e_S(\frac{17.269}{237.3+T})(1 - \frac{T}{237.3+T})$ where all the variables are as described in equation 15 above. The Penman Monteith equation was now be able to be modelled based on the available meteorological data for the area.

The cultural evapotranspiration which represents the real value of the evapotranspiration occurring under the actual weather conditions, growth stage and soil calculated from:

$$ET_c=K_cET_0 \qquad (16)$$

Where

ET_c is cultural evapotranspiration and K_c is the cultural coefficient estimated depending on the growth stage of the plant to be irrigated.

The effective precipitation is dependent on the soil management, soil characteristics and the quantity of the precipitation received. They determine the amount of precipitation that remains near the rootzone of the crop without deeply percolating. The difference between the cultural evapotranspiration and the effective precipitation P_{eff} is the crop water requirement (CWR). Using the USDA-SCS method for estimating effective precipitation, P_{eff} was calculated as 80% of the actual rainfall. Additional water is required to cover for the efficiency of the crop in using the water (irrigation efficiency, η_i) and to get rid of salts (leaching requirement, LR)

From these, the daily water requirement was determined from

$$\text{WR} = \frac{CWR}{(1-LR)\eta_i} \quad (17)$$

3.1.7 Pumping system

The pumping system is based on the amount of energy required to deliver the daily water requirement. Excluding any efficiencies, the hydraulic energy required at the outlet of the pumping system is expressed as (Glasnovic & Margeta, 2007b):

$$E_h = \rho g Q H_{TE} \quad (18)$$

Where E_h represents the hydraulic energy. This is directly affected by Q, the volumetric amount of water pumped daily, H_{TE} the total head, g the acceleration due to gravity and ρ, the density of water.

The power required by the pump in kW was estimated using the equation:

$$P_p = \frac{\rho g Q H_{TE}}{\eta_P \times 10^3} \quad (19)$$

Where η_P represents the efficiency of the pumping unit (the motor and the pump)

3.1.8 PV system sizing

The irrigation water requirement calculation yields the volumetric amount of water to be pumped daily. Together with the total head, the daily hydraulic energy will result. The PV system could now be sized basing on the equation (Campana et al., 2013):

$$P_{max} = \frac{E_h}{I\eta_s} \quad (20)$$

Where: P_{max} is the peak power to be derived from the PV array,

E_h the total daily hydraulic energy required

I represent the mean daily radiation on the surface of the array

η_s is the system efficiency that incorporates the efficiencies of the components: the pump, the solar array, the inverter, and losses e.g. system losses and friction losses etc.

3.1.9 System simulation

The solar insolation reaching the earth and falling on the surface of the Solar array is a cumulative sum of three components; the direct (beam), diffuse radiation stemming from scattering of the light by the atmosphere and the reflected ground radiation. They can be represented as:

$$I = I_b + I_d + I_r \tag{21}$$

Where I, I_b, I_d, I_r represent the total, beam, diffuse and reflected radiation respectively.

The total horizontal radiation received is computed to obtain values on the tilted surface according to:

$$I_t = \frac{I_{gh} - I_{dh}}{\cos(90-\alpha)} \cos(\theta) \tag{22}$$

I_t, I_{dh}, I_{gh} are the global total radiation, the global horizontal radiation and the diffuse horizontal radiation respectively.

The angle of incidence (θ) is defined according to the equation:

$$cos\theta = cos\theta_z cos\beta + sin\theta_z sin\beta \cos(\gamma_s - \gamma) \tag{23}$$

Where θ_z

β this is the slope of the surface on which the solar array is installed

γ_s is the solar azimuth angle

γ is the surface azimuth angle

The power generated by a PV array is a factor of the solar insolation, technical characteristics of the cells and the cell temperature. With an MPPT tracker, the solar module operates at the maximum point.

To determine the power generated by the photovoltaic array we must factor in the equation that is dependent on the normal operating cell temperature and the efficiency under standard test conditions

The power generated by the array is thus given by:

$$P_{PV} = \frac{I}{1000W/m^2} P_{ref}(1 - \alpha(T_C - T_{ref})) \quad (24)$$

Where I is the solar insolation

P_{ref} is the nominal power of the PV array. This is taken as the power of the PV module with the standard test conditions of: peak radiation of $1000W/m^2$, reference temperature of 25ºC, relative air mass of 1.5

α is the temperature coefficient of the solar cell

T_{ref} is the reference temperature of the solar cell

The temperature coefficient and the deviation of temperature from the reference temperature is to highlight the reduction in efficiency of the PV module with an increase in cell temperature. This is an implicit equation stemming from the equation of efficiency

$$\eta = \eta_{ref}(1 - \alpha(T_C - T_{ref}) + \gamma logI \quad (25)$$

The cell temperature is affected by the ambient temperature and the normal operating cell temperature (NOCT) according to:

$$T_C = T_a + (T_{NOCT} - 20^0C)\frac{I}{800W/m^2} \quad (26)$$

The total power generated from all the PV arrays installed is dependent on the efficiency of the PV modules, the total surface area of the PV arrays and the total irradiance received. Thus,

$$P_{PV} = \eta A I_t \quad (27)$$

Where η, A and I_t represent efficiency of the PV modules, the surface area of the PV array and the total irradiance respectively

Crop yield Simulation Models

According to Gommes (1998), crop weather yield simulation models are used to predict the production of crops as a result of changing weather conditions. This can be due to changing weather conditions, pattern changes from technology application and improved practices and crop management practices such as disease and pest control. In Sub-Saharan Africa where technology uptake is still low, yield variability is most correlated with weather conditions and crop management practices.

Several crop simulation models exist in literature for prediction of crop yield, effect of management practices, water response, mass balances etc. These models can be categorized as statistical, mechanistic and functional simulation models (Basso, Cammarano, & Carfagna, 2013).

Statistical methods were the first to be used and show the trend of productivities of lands over a period of time using regression. It has shown the increase in crop productivities over several past years. This has been attributed to the effect of technological advancements over the last couple of years such as genetics, improved crop management practices etc. Mechanistic models, on the other hand, try to model the various biological processes of plants such as photosynthesis and transpiration to predict the yield. Functional models try to make crop modelling simple by using empirical formulas.

The crop simulation models have been packaged into applications. These include APSIM, AquaCrop, DSSAT, hybrid-maize, CropSyst, ADEL among others which have been used with great effect and robustness in the prediction of maize yields. The main aim of this study is to predict the crop yield as a result of the irrigation practices, soil water conditions, environmental variations. Most of the other models, e.g. Hybrid-Maize and WOFOST are location specific, they have been calibrated only for use in the US and Europe.

AquaCrop was developed by the Land management division of FAO (2016) in an effort to predict the reduction in the productivity of crops as a result of water supplied to the crop. The crop yield for the maize as from the irrigation supplied, the climatic conditions, and the soil characteristics was predicted using the equation proposed in FAO irrigation and drainage paper 33 outlined below:

$$\left(1-\frac{Y_a}{Y_x}\right)=K_y\left(1-\frac{ET_a}{ET_x}\right) \tag{28}$$

Where Y_a, ET_a represent the actual values of yield and evapotranspiration while ET_x, Y_x represent the optimum values respectively. K_y represents the factor that correlates the reduction in evapotranspiration to the corresponding reduction in the yield of the crops. It quantifies the reduction in yield due to water deficits. AquaCrop will give an output of biomass production and yield production in tons per hectare. This was used to determine the revenue from the farming practice from the sale of maize grain produced.

Hydraulic System

Narvate Lorenzo and Caamano (2000) proposed to define the total dynamic head of borehole water pumping system from;

$$H_{TE(i)} = H_{OT} + H_{ST(i)} + \frac{H_{DT(i)} - H_{ST(i)}}{Q_{max}} Q_{AP(i)} + H_{F(i)}(Q_{AP(i)}) \quad (29)$$

Where i represents the time steps, $H_{TE(i)}$, H_{OT}, $H_{ST(i)}$, $H_{DT(i)}$ and $H_{F(i)}$ represent the total dynamic head, the head difference between outlet and ground surface, static water level head, dynamic water level in the borehole, and friction loss head respectively. Q_{max} and $Q_{AP(i)}$ represent the maximum yield from the borehole and the flow rate at the given time. The total dynamic head therefore is comprised of the fluctuating values of the dynamic level and actual flow. The actual flow in the dynamic system changes with the power delivered to the pump.

Borehole Modelling

The water level in a borehole is not constant but falls as a result of water being drawn. The rate at which it is being drawn partially determines the drawdown level. Narvate et al. (2000) in his experiment to analyse PVWPS from boreholes appreciated characterization of boreholes using pump tests. During the test, the water is drawn using a constant pumping rate system until the level has stabilized to determine the drawdown level of the borehole. It is therefore paramount to determine the borehole characteristics after it has been set up. Pumping tests provide also the maximum discharge rates from the boreholes as a preventive measure against overexploitation of the ground water resources.

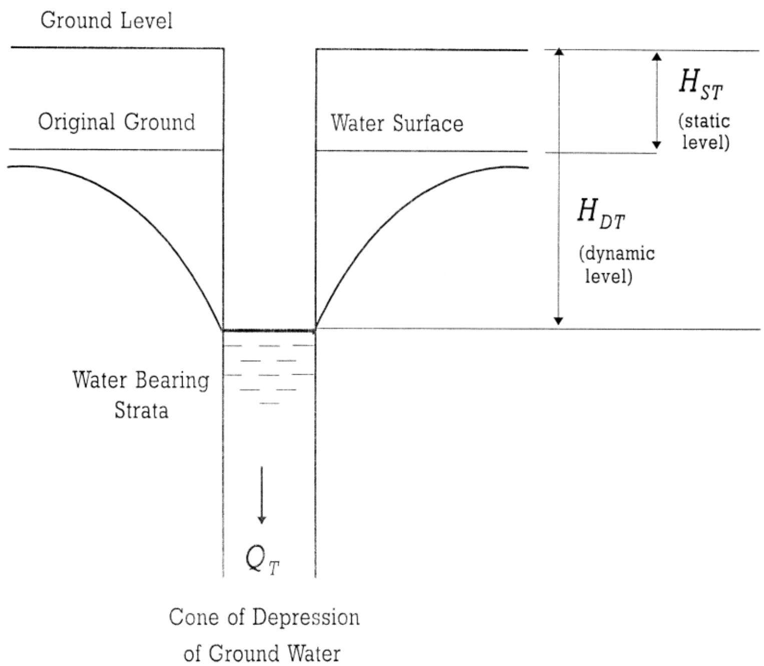

Figure 9: Dynamic Ground Water Level (Narvate et al., 2000)

The dynamic water level modelled follows the equation that stems from the consideration that the pumped water will make the water level drop while refilling of the borehole from the surrounding raises the level. It follows then that the dynamic level can be modelled using

$$\frac{dHD}{dt} = -\frac{1}{\tau} \times HD + \frac{Q(t)}{A_w} \quad (30)$$

Where τ and A_w represent the recovery time and cross-sectional area of the borehole respectively. Under steady state conditions, $dHD/dt = 0$, and therefore (30) solves to

$$HD = \frac{HD_{ref}}{Q_{ref}} \times Q \quad (31)$$

where HD_{ref} *and* Q_{ref} represent the drawdown and discharge at the reference or test conditions (Mermoud, 2004). The ratio of the two parameters is specific to boreholes and is referred to as the specific drawdown.

Friction Loss

Fluid flow in pipes undergoes resistance due to the effect of the surface roughness of pipes. This depends on the finishing of the internal surfaces of pipes, age of use of pipes and on the type of material used in manufacturing the pipes and fittings. Rough surfaces and older pipes exhibit higher resistance to fluid flow as compared to smooth and new surfaces (Ntengwe, Chikwa, & Witika, 2015). The head losses are also enumerated to include losses from inlets, exits, valves, elbow and bends all summed up in the equivalent length. The effect of these losses is that additional energy is required to cater for the losses and hence deliver the fluid to the desired destination.

The common formulas used to quantify the friction losses are Darcy-Weisbach, Moody, Manning and Hazen-Williams equations. Mostly though, the Darcy-Weisbach and Hazen-Williams pipes are used. They are very related in their formulas as shown below

$$h_L = \frac{C"LQ^2}{D^5} \quad (32)$$

$$h_L = \frac{10.77L}{D^{4.865}}\left(\frac{Q}{C_{hw}}\right)^{1.852} \quad (33)$$

Where h_L, L, D, Q and C represent the friction loss head, pipe length, pipe diameter, fluid flow and pipe loss factor.

From the formulas, it is evident that the friction loss, h_L, is directly proportional to the length of the pipe and the square of volumetric flow rate but inversely proportional to the fifth power of pipe diameter (Ntengwe et al., 2015; Richardson and Coulson, 1999). It is paramount to compute this as it contributes in reducing the efficiency of pumps since the flow rate reduces with increased total effective dynamic head. The effective friction loss in solar ground well pumps fluctuates due to the change in the well water level and the pumping rate resulting from solar energy available from the solar array during the day.

During simulation, the system parameters are adjusted taking the parameters and time durations of an hour. These are input in three software tools that will be used. CROPWAT tool is used to simulate crop water requirements under various input parameters of temporal and local conditions. Microsoft Excel, PVSYST, and MATLAB are used in dynamic modelling of the system to evaluate the sized system. The crop yield depends on the parameters of soil, weather conditions and water supply. With these, the produce is simulated using AquaCrop.

3.1.10 Economic assessment of PVWP system

In this section, the profitability of the system is determined throughout the lifetime of the project factoring in discounting and inflation rates. It is performed using the economic indicators of Net Present Value (NPV), Payback time, and internal rate of return. A comparison is then done to determine the most profitable system between PVWP and diesel pumping system.

Before the economic indicators are used to analyse their profitability, the component costs and longevity have to be obtained. The lifespan of each component is important as this will help in determining the number and cost of replacements before the lifetime of the entire system elapses (Kenna and Gillet, 1985). It is important to the investor to have this information beforehand so as to make decisions on options to financing, planning replacements etc.(Shrestha et al., 2014)

The potential benefits and competitiveness of PVWP depends on upfront costs, maintenance and operation costs, accruing benefits or revenues generated and current cost of power (IRENA, 2016a)

$$LCC = IC + O\&M + FC \tag{34}$$

Where LCC, IC, O&M, and FC represent the Life cycle costs, initial costs, operation and maintenance costs and fuel costs respectively. All the values are the present values after discounting. The economic indicators were derived according to the equations:

The net present value represents the value obtained from the difference in the cumulative cashflows obtained during the lifetime of the project discounted to the current period and the initial capital costs incurred

$$NPV = \sum_{i}^{n} \frac{CF_i}{(1+r)^i} - ICC \tag{35}$$

Where NPV is the net present value

CF being the cashflow being the difference in the revenue generated and the expenses incurred in year i

n is the final year of the project

ICC is the initial capital costs

r is the discounting rate

The internal rate of return (IRR) represents a discounting rate which when applied brings the NPV to zero. The higher the IRR the more profitable the project is. It is compared to the cost of finance and if it is higher, the project is deemed financially viable.

IRR is obtained by equating the NPV to zero and solving for the r in the NPV equation

$$0 = \sum_{i}^{n} \frac{CF_i}{(1+r)^i} - ICC \qquad (36)$$

Payback time,

$$PBT = \frac{ICC}{CF} \qquad (37)$$

It represents the time it takes to recoup the initial capital invested in the project

CHAPTER 4: RESULTS AND DATA ANALYSIS

This section presents the results obtained from the analysis of the climatic data, system design and the hourly dynamic simulation of the overall system. It also incorporates the economic analysis of the SPIS and its comparison with the DPIS.

4.1 Climatic conditions of the area

The average monthly temperatures in the area range from 25-31 ^{0}C. Instantaneous temperatures in the area fluctuate with low values of 20 ^{0}C and highest values of 38 ^{0}C. Considered an arid climate under the agricultural economic zones of Kenya, the area receives an annual rainfall of 385 mm while some parts of the country receive precipitation as high as 1800 mm. Saretho has two rainy seasons, March to May and October to December with the highest rainfall being received in the months of April and November both at around 80 mm, the long rains being during the latter. In fact, half of the annual rainfall is received during the months of October through to December. It is exhibited in Figure 10 and Figure 11.

Figure 10: Kenya Agro-ecological Zones (AEZ)

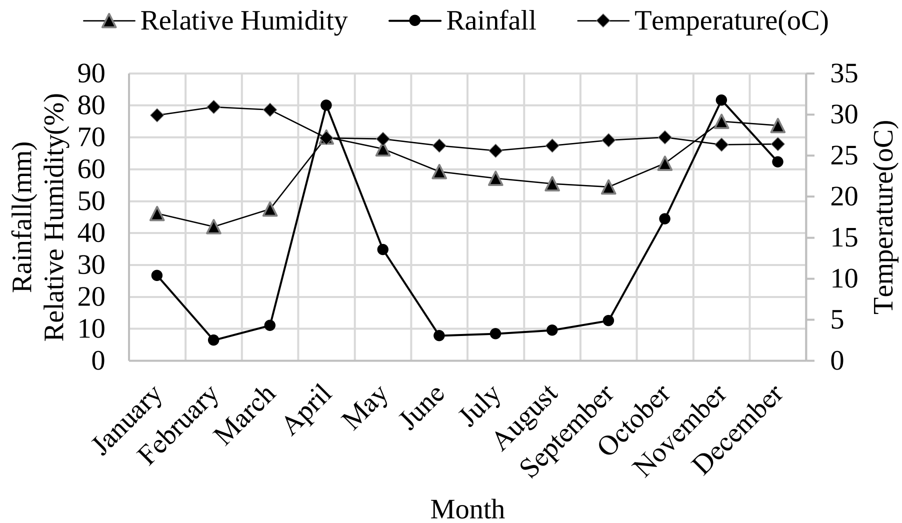

Figure 11: Weather variation in a year

The monthly data for relative humidity, wind speed, rainfall, irradiation and Temperature for Saretho, Garissa, Kenya are shown in Table 1. They were used in the preliminary design of the water pumping system and estimation of the daily water requirement by the maize crops under irrigation on a 1-hectare piece of land.

Table 1: Average Monthly meteorological conditions and Irradiation

Month	Relative Humidity (%)	Wind speed (m/s)	Rainfall (mm)	Irradiance (W/m^2)	Temperature (^0C)	Irradiation ($kWh/m^2/Day$)
January	46.19	3.64	26.68192	230	29.9	5.520
February	42.01	3.67	6.413083	240	30.92	5.760
March	47.58	3.74	11.09971	242	30.59	5.808
April	70.13	4.33	80.07008	229	27.16	5.496
May	66.37	5.56	34.8026	221	27.04	5.304
June	59.32	7.69	7.844807	200	26.2	4.800
July	57.16	7.93	8.40758	194	25.6	4.656
August	55.44	7.81	9.54616	213	26.21	5.112
September	54.5	7.88	12.51964	219	26.88	5.256
October	61.93	5.78	44.41295	241	27.21	5.784
November	75.01	2.36	81.68321	213	26.32	5.112
December	73.72	2.05	62.25451	218	26.39	5.232

Soil characteristics

The area has slightly alkaline soils with a PH of 7.4 and low organic matter. The soils thus have a low infiltration and water holding capacities. The soils are also low in micronutrients of potassium, magnesium, manganese, phosphorus, and copper. Application of acidifying fertilizer rich in phosphates and ammonia such as Di-ammonium Phosphate (DAP) was proposed by the Ministry of Agriculture for the area(NAAIAP, 2014). Enrichment of the soil using manure has also been recommended. The application rates are:

Table 2: Fertilizer application rates (NAAIAP, 2014)

Manure	8 t/ha
Planting	125 kg/ha CAN
Top dressing	200kg/ha CAN

4.2 Design of Solar Water pumping for Irrigation

4.2.1 Irrigation water requirement

The daily irrigation water required by the crop is dependent on the stage of the crop, the soil parameters, and the environmental conditions.

The soil conditions, the stage of growth and type of crop are summed up in a cultural evapotranspiration coefficient, Kc, as provided by FAO. The figure indicates the Kc values for maize under the different growing stages in arid climates.

Table 3: Cultural Coefficients of maize

Growth stage	Initial Stage	Development Stage	Mid-Season	Late Season	**Total**
Days	25	40	45	30	**140**
Kc	0.3	0.8	1.2	0.35	

From the table, it is deduced that the maize will take nearly five months (140 days) to mature. To reduce the irrigation water requirement, the maize is timed to coincide with the long rainy season which occurs in the months of July to November in the area with the planting date set for the 3rd of July or thereabouts.

The initial stage was applied to July and August, mid-season extending into October and the late season happening in November.

The reference evapotranspiration from the FAO Penman-Monteith equation combined with the cultural coefficients in Table 3 resulted in IWR of the maize crop as shown in Figure 12. It has a big dependence on the amount of rainfall.

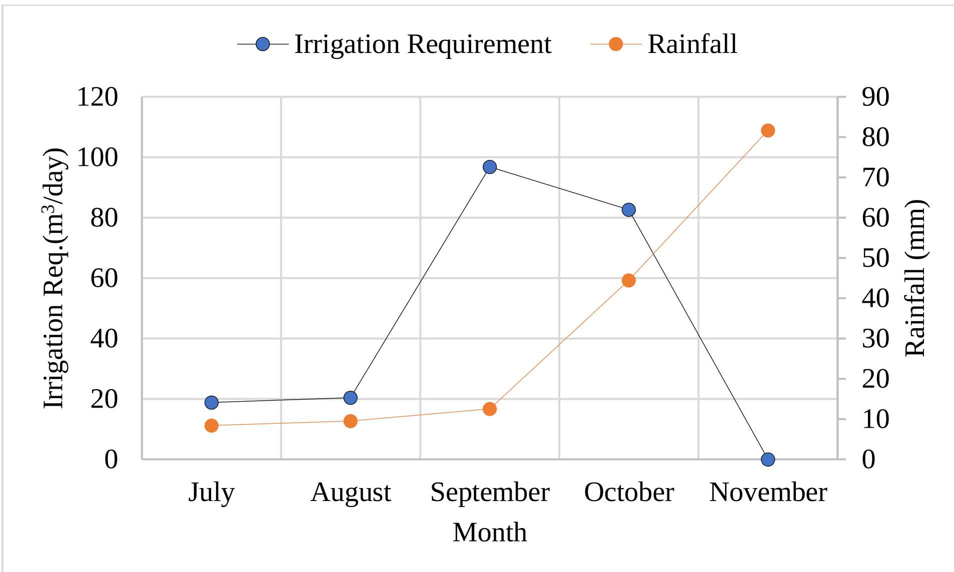

Figure 12: Irrigation water requirement variation

The amount of water required for irrigation is the shortfall in the difference between the cultural evapotranspiration, Kc, and the effective rainfall. Figure 12 shows the variation of irrigation requirement during the growing season of the crop. The highest water demand is experienced during the month of September reaching a high 96.8 m^3/day with the month of November representing the no water demand. This results from low rainfall during the month of September and peak rainfall during the month of November that surpasses the crop water requirement. September is also the mid-season stage of development with high water requirements as indicated by the peak value of the cultural evapotranspiration coefficient K_C at 1.2.

The weather parameters interact in various effects to evapotranspiration which is the main component of crop water requirement.

The month of September is seen to have the lowest rainfall, highest wind speed and lowest relative humidity in the growing season. In combination, they increase the reference evapotranspiration. Increased wind speed transports the already evaporated and transpired water vapour from the soil and leaf surface respectively thereby increasing the vapour pressure gradient and create more space for water vapour to evaporate to. Therefore, an increase in wind speed increases the evapotranspiration. Temperature has the same effect caused by a reduction in the vapour density making it easier to be displaced by evapotranspired water molecules.

Relative humidity has the effect to inhibit the crop losing water to the atmosphere. This is because as the humidity increases, the vapour pressure concentration increases making the air more saturated (Brown, 2014).

4.2.2 Solar Resource

The yearly average of solar irradiation in Saretho is 5.32 kWh/m^2/day. The values, however, vary from lowest irradiation received in the month of July of 4.65 kWh/m^2/day to the highest irradiation, experienced in the month of March of 5.81 kWh/m^2/day as shown in Figure 13

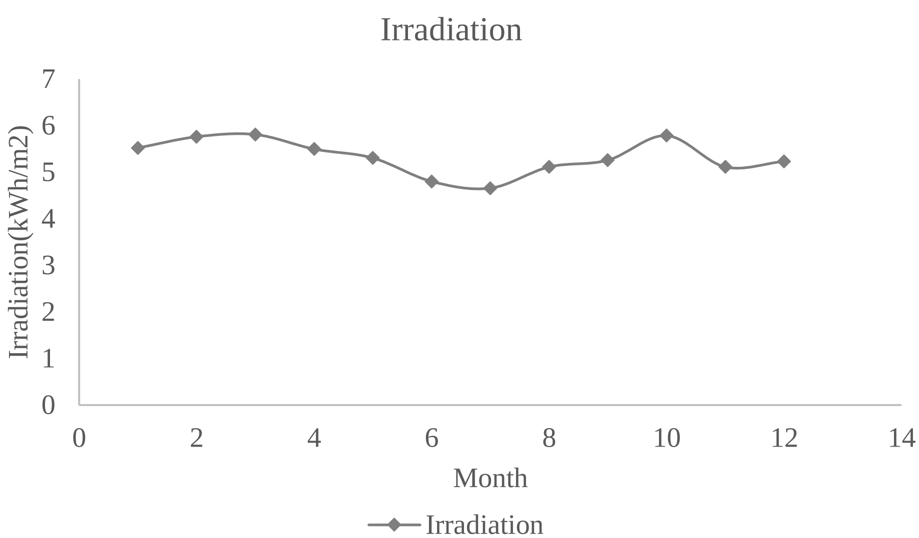

Figure 13: Monthly daily average irradiation

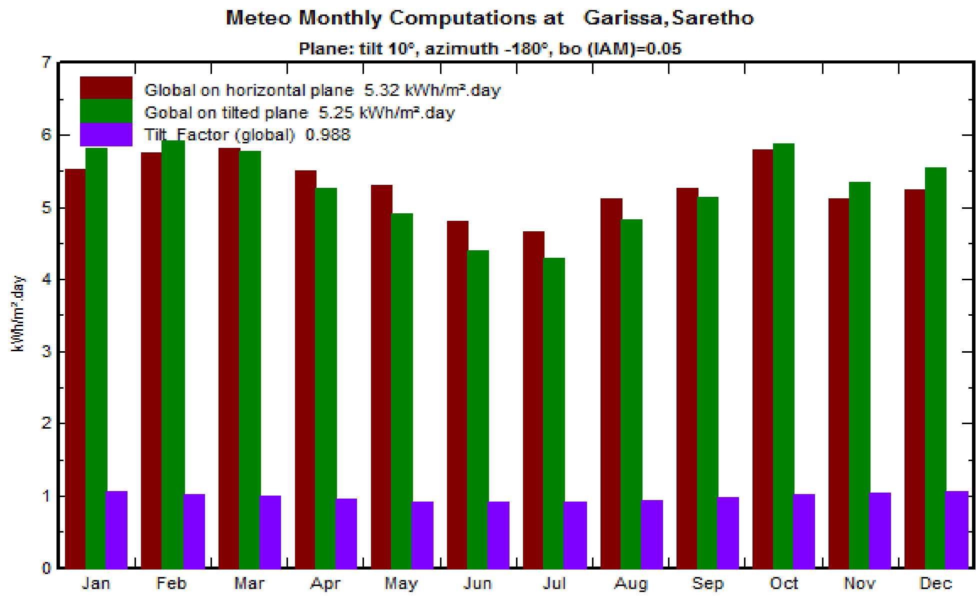

Figure 14: Optimization of angle of inclination

Using PVSyst software to optimize the orientation of the Photovoltaic plane, it is observed that the optimum values for the location are obtained when the PV array is fixed at the horizontal. The irradiation is analysed for both fixed mounted plane and fixed tilted system. At an average of 5.32 kWh/m^2/day, the horizontal system receives more radiation than the tilted system. The average global radiation on the tilted surface reduced as the tilt angle reduces. At a tilt angle of 10^0, it receives an average global irradiation of 5.25 kWh/m^2. The optimization is shown in Figure 14.

4.2.3 System design

The preliminary design was based on the worst month scenario when comparing the solar radiation available and the hydraulic energy required to pump the water. The worst month scenario was determined considering the month with the highest analysed ratio of hydraulic energy required to pump the water and the available average solar insolation

Table 4: Design month determination

Month	July	August	September	October	November
Irrigation Req. (m^3/day)	23.44	25.60	116.48	115.33	0
Irradiation Horizontal (kWh/m^2/day)	4.656	5.112	5.256	5.784	5.112
Ratio	198.6	199.7	45.1	50.1	Inf.

Comparing the values of irradiation against the irrigation water requirement, September has the lowest ratio indicating a high stress month. This is taken as the design month. The rationale is that, since the system is able to supply the irrigation water demand during the most stressful month, it is able to cover the other months.

The hydraulic energy required to overcome to deliver the irrigation water requirement per day is dependent on the hydraulic head and the water requirement. It is equal to the potential energy if all the water were at the destined point in reference to the pumping position.

The borehole in Saretho, which lies on the Merti aquifer has the parameters shown in Table 5

Table 5: Borehole characteristics

Diameter (mm)	HD_{ref} (m)	Q_{ref} (m^3/h)	HD_{ref}/Q_{ref} ($m/m^3/h$)
100	3.1	16	0.2

The hydraulic energy required to pump this water to a maximum hydraulic water head of 40 m is calculated as:

$$E_h = \frac{\rho g Q H_{TE}}{3600} = \frac{1000 * 9.81 * 96.8 * 40}{3600 * 1000} = 10.55\ kWh/day$$

The size of PV panels required to cater for this demand is determined by the size of the irradiance at the area and the overall efficiency of the system. For sizing calculations, the system efficiency is a combination of efficiencies of the various components in the system. The system efficiency is directly proportional to the efficiency of the PV modules, inverter efficiency, pump efficiency and the irrigation efficiency. The water requirement, however, has taken consideration of the irrigation efficiency in determining the crop water requirements.

The overall system efficiency is therefore comprised of these efficiencies according to equation 38 below:

$$\eta_S = \eta_P * \eta_i * \eta_{PV} \qquad (38)$$

Where $\eta_S, \eta_P, \eta_{PV}$ are the pump, inverter and PV module efficiencies

The peak power from the PV array was obtained as

$$P_{peak} = \frac{E_h}{I * \eta} = \frac{10.55}{5.256 * 0.35} = 5.7\ kWp$$

The pump is assumed to operate for a duration of 7 ½ hours per day. Therefore, to obtain the power of the pump, the total daily water demand is presumed to be pumped during these operating hours. The pump power is subsequently calculated as

$$P_P = \frac{\rho g Q H_{TE}}{\eta_P} = \frac{1000 * 9.81 * 96.8 * 40}{3600 * 1000 * 7.5 * 0.45} = 3.2\ kW$$

A 200 Wp monocrystalline PV module model Dayliff YL200 from Davis and Shirtliff East Africa with an efficiency of 15.73% is chosen. The module parameters are in the appendix.

The array area is affected by the efficiency of the PV modules, the power requirement, and the total peak insolation. The array area is obtained from the equation $P = \eta_{PV} A I_t$

Thus, $A = \frac{5.7}{0.1573 * 1000} = 37\ m^2$

The design parameters were summarized in the table below:

Table 6: System Design Parameters

Irrigation water requirement (m^3/day)	96.8
Irradiation(kWh/ m^2/day)	5.256
PV peak power (kWp)	5.7
Power of the pump (Kw)	3.2
Pump Operating time (hrs.)	7.5
Model of the PV module	Dayliff YL200
Model of Pump	Lorentz PS4000 C-SJ8-15 pump with controller
Module efficiency (%)	15.73
Array area (m^2)	37

System Simulation and optimization

In order to determine differences in the instantaneous supply and load requirements of the system, dynamic system simulation of the whole system was done. The simulation utilized hourly meteorological and irradiance data for the design month of September and for the whole season.

To optimize the system, a comparison was made between the water demand and supply with a view to match them.

4.3 Effect of Weather conditions on the irrigation water requirement

4.3.1 Irradiation

As compared to the monthly averages where variations range between 9-12% from the annual averages, hourly values oscillate from day values and night values. Irradiation has the highest variation from maximum day irradiances at around noon to no irradiance received at night. Temporal weather fluctuations during the day for irradiances are also expected given the variation in the clearness indices caused by the position of the sun, shading, cloud cover, humidity, dust storms (especially desert like conditions) and particle presence in the atmosphere.

The variation of irradiance during the day has a contributing effect on the evapotranspiration. It is therefore noted that the values of reference evapotranspiration move almost in tandem with the solar intensity.

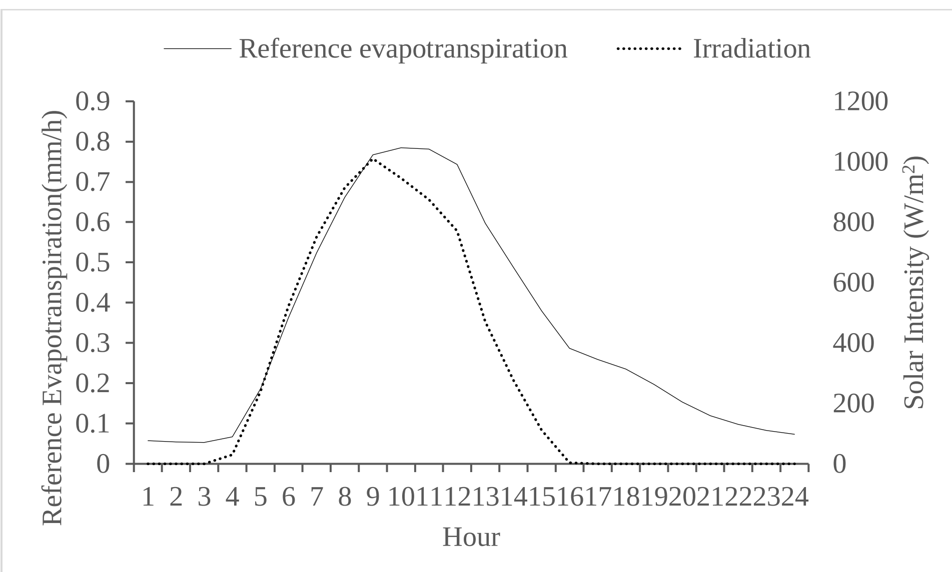

Figure 15: Effect of Solar Intensity on Evapotranspiration

From Figure 15, of ET_O and solar intensity during a normal day in the month of September, the highest loss of water by the plant is during around mid-day. This is exhibited by ET_O value of 0.8 mm/h. In modelling of the reference evapotranspiration, the solar term is significant. This follows from the fact that the main source of energy responsible for vaporizing the water from the surface of the plant is the solar energy. Some energy, however, is used to raise the temperature of the soil and thus the reducing component of the soil heat flux. During the times when the sun has set, there is residual evapotranspiration from highest just after sunset and lowest before sunrise. Immediately after sunset, the water loss is still dependent on the residual heat from irradiation in the soil and in the atmosphere. The temperature reduces and is lowest just before sunrise.

Wind speed during variation is significant as demonstrated by Malek (Malek, 1992). The day experiences higher average wind speeds in the area. In combination with the solar intensity, the irrigation water requirement is higher. Figure 16 illustrates the significance of wind speed in its contribution to irrigation water requirement during a day on the farm.

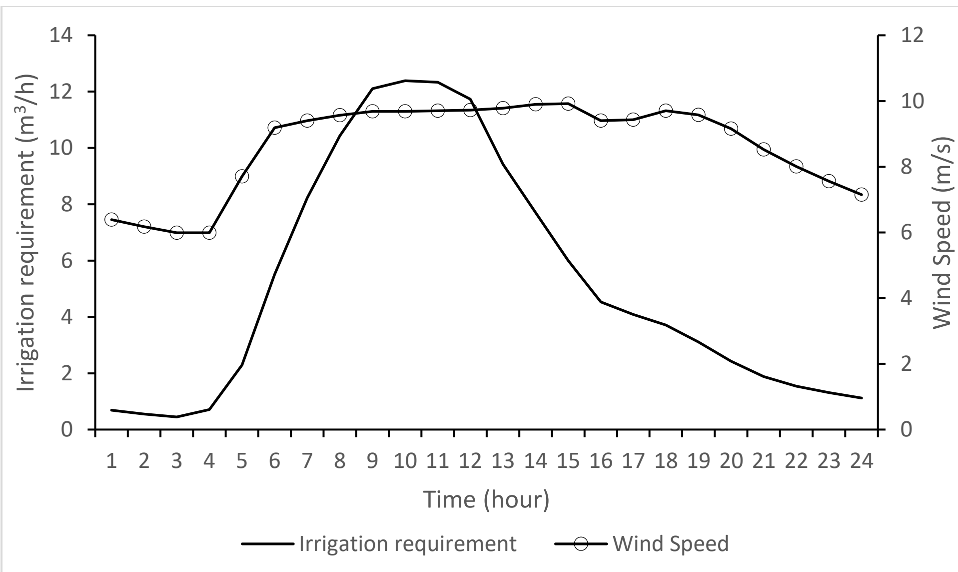

Figure 16: Wind Speed Variation with IWR during the day

The irrigation water demand is therefore seen to vary greatly with the environmental conditions. The pattern established however is consistent with the solar intensity. This is important in the feasibility of using solar water pumps.

4.3.2 Temperature effect on PV panel performance

The performance of the PV module is dependent on the module parameters (material, operating temperature, temperature coefficient etc.), the irradiance and the ambient temperature. Both irradiance and temperature vary throughout the year. The effect of temperature and irradiance variation on the performance of the PV module is depicted in Figure 17.

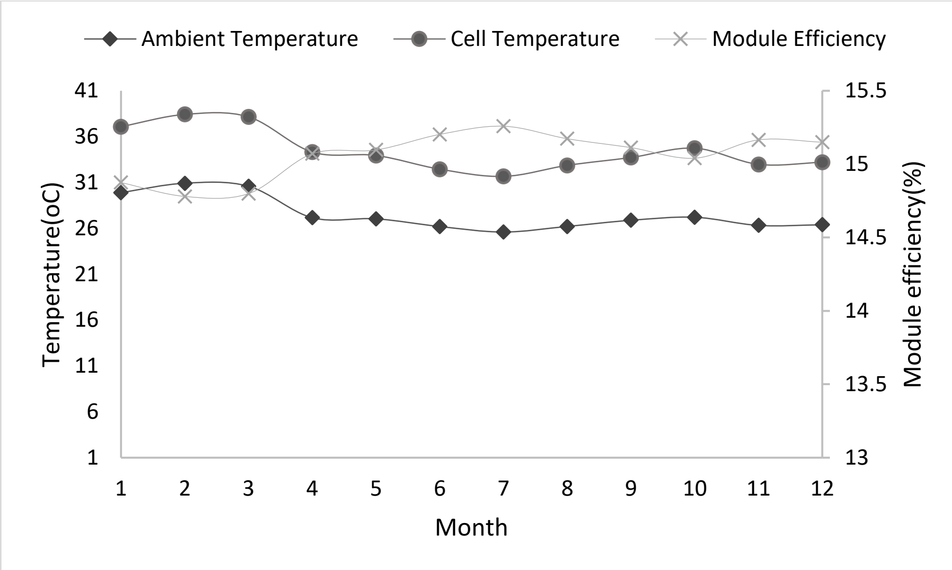

Figure 17: Effect of Temperature on Module performance

The efficiency of the module is observed to be closest to the optimum module efficiency in the month of July and lowest in March. The cell temperature is seen to be mostly dependent on the ambient temperature. The largest loss in efficiency is experienced in March registering a drop 6%. In combination, however, the hottest months experience the highest solar irradiance at 242 w/m^2 in March. It can, therefore, be deduced that the increase in temperature has an effect of lowering the efficiency of the PV module efficiency.

The decrease in efficiency due to temperature increase is explained by the reduction of the band gap of the semiconductor material and hence reduces the electric field which is essential for the creation of a potential difference across the PV cell. Increase in recombination rates of the carriers has an effect of reducing their concentration. (Dubey, Sarvaiya, & Seshadri, 2013). Temperature changes, therefore, have a high effect on the voltage of the module.

During the day, the performance of the PV array changes due to temperature fluctuation. Increase in temperature increases the cell temperature. For the PV panel selected, its power output during a typical day in September is shown in Figure 18.

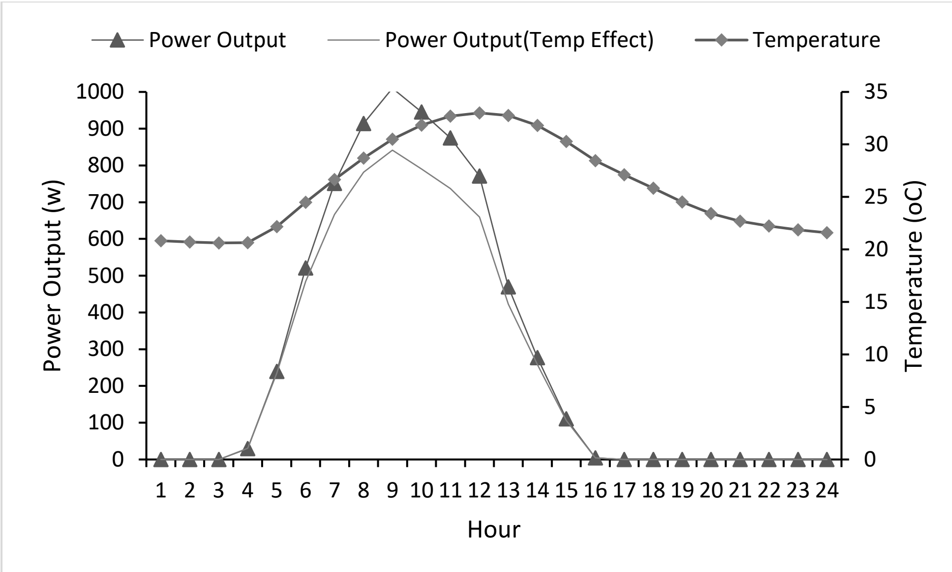

Figure 18: Hourly power Output of PV with temperature effect

During the period in the middle of the day, the efficiency of the PV module decrease so does its output. This is shown to be strongly affected by temperature. High temperatures during the day reaching 34 ^{0}C reduces the production of the PV module from an ideal capacity by margins up to 16%.

The power output from the installed solar PV system will, therefore, follow the characteristic curve of the 1 kWp module demonstrated above. According to Khatib (Khatib, 2010), the power produced from the PV array is obtained as:

$$P = \frac{\rho g H Q \eta_r}{G_T \eta_{PV} \eta_s} \tag{39}$$

where Q, η_r, η_{PV}, η_s represent the quantity of water delivered, the efficiency of the PV panels at reference conditions, the efficiency of the PV panels at operating conditions and the system efficiency respectively. Reduction in the power production of the PV panels had the effect of reducing the quantity of the power delivered to the pump according to the equation 39 above. When this happens, by extension, the quantity of irrigation water delivered by the pump is reduced. To cater for this, when there are mismatches, it may necessitate addition of an extra PV panel.

4.3.3 Hourly Water Demand

Precipitation and evapotranspiration play the greatest role in the irrigation water requirement. The soils infiltration capacity, irrigation efficiency and the leaching requirements too come in effect to increase the amount of water to be supplied to the field.

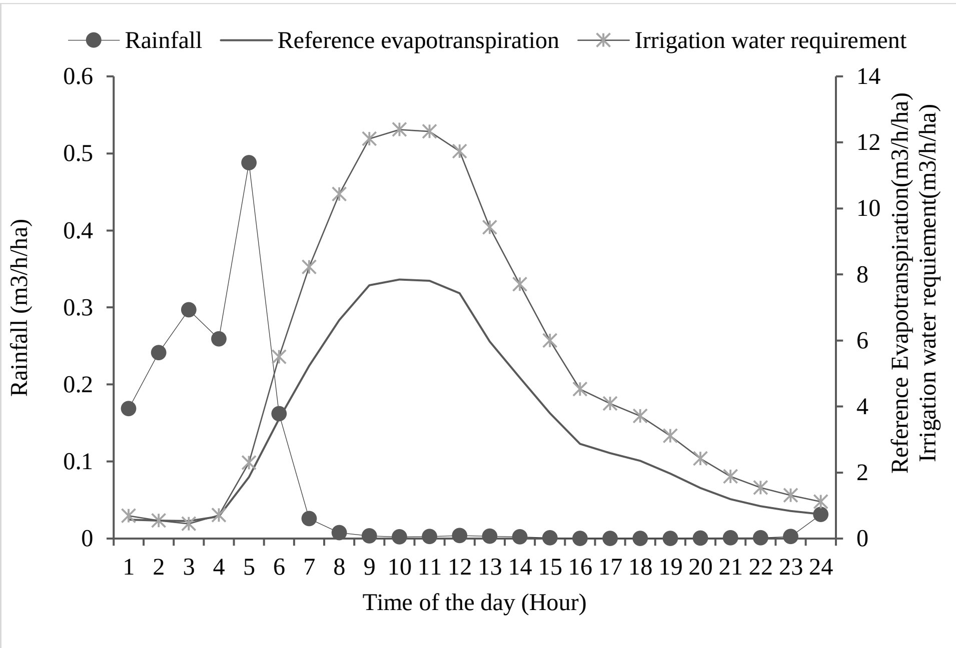

Figure 19: Water demand components

The precipitation during the month is very low. In a typical day of the month, precipitation is seen to occur after midnight with the highest rainfall on the 1-hectare piece of land being in the tune of a meagre 0.5 m^3 per hour. Compared to reference evapotranspiration of 8 m^3/hour, the water deficit required by the crops is large. Factoring in the irrigation efficiency of the drip irrigation system, the cultural coefficient, and the leaching requirement, the highest water requirement to be supplied to the piece of land reaches around 12 m^3 per hour. The pump selected was, therefore, the one that would be able to deliver this quantity of water in an hour (peak discharge).

Pumped water simulation

The water that is pumped is modelled with reference with the hydraulic head and the power input from the PV solar array. Given the small fluctuations in the dynamic head as a result of the small-time steps and to simplify the modelling of the quantity pumped, the total head is taken as more or less constant. As such the pump characteristics taken from the data of flow rates and input power at the pump height is plotted in excel and the curve is fitted to yield the 4^{th} degree polynomial.

$$Q = aP^4 + bP^3 + cP^2 + dP + e \tag{40}$$

The curve fitting is summarized in Table 7: Pump fitting results

Coefficients (with 95% confidence bounds):

Table 7: Pump fitting results

a	-2.6×10^{-13}		
b	2.24×10^{-9}		
c	-7×10^{-9}		
d	0.01292		
e	-2.486		
Goodness of fit			
SSE	R-square	Adjusted R-square	RMSE
0.05127	0.9996	0.9978	0.2264

The equation was used to simulate the flow of water during the day as the solar intensity changed together with the power supply from the PV array.

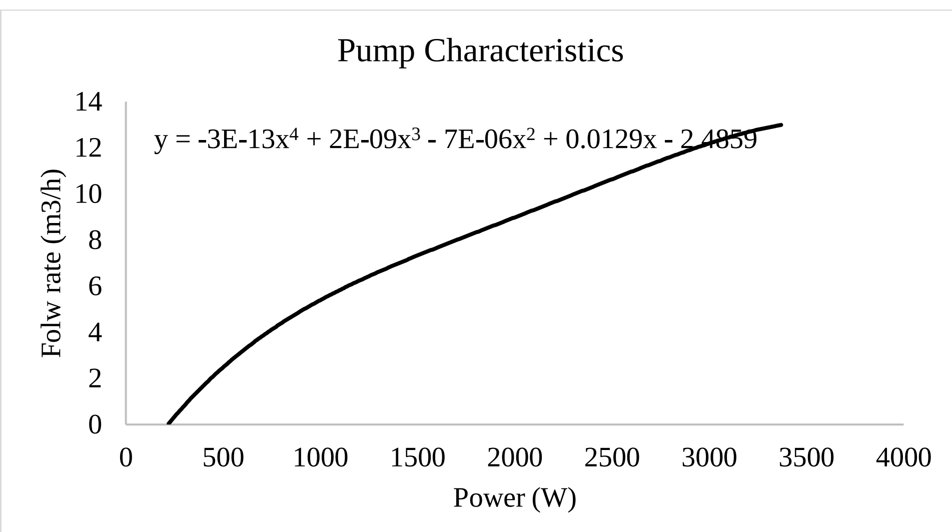

Figure 20: Pump characteristic curve

From the curve in Figure 20, the maximum flow rate with the total head at 40m occurs at $13m^3/h$ when a power input of 3.4 kW is delivered to the pump. A cut in power of 220W is required below which there will be no discharge delivered by the pump. Also, since the rated capacity of the pump is 3.4kW, a flow rate 13 m^3/h was taken as the maximum discharge should the power output by the PV array exceed 3.4 kW.

The main goal of simulating the performance of the system is to understand if the system designed can meet irrigation demand throughout the life of the crop. The water pumped by the pump at the given climatic conditions was compared to the water demand at the given hourly, cumulative daily, monthly and the whole planting season as both the water demand and the performance of the PV modules are subject to environmental conditions. The overall system performance was therefore achieved through the simulation.

In a typical day in September, representing the 65th day after planting the crop, the irrigation water requirement versus the water supplied can be summarized in Figure 21:

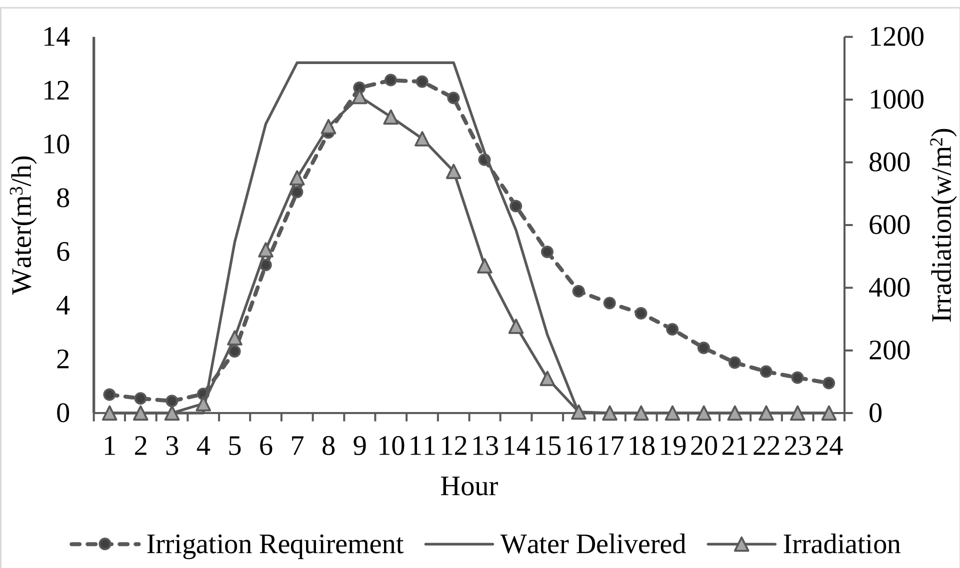

Figure 21: Hourly water delivered and IWR

From the graph, it can be deduced that the water being pumped during the period when there is sufficient irradiation surpasses the irrigation water requirement. The maximum water delivered, however, peaks as the solar intensity peaks in the middle of the day. In the afternoon past 14 hrs, the amount of water delivered starts becoming less than the irrigation requirement. The water requirement by the crop past the point is in excess of the supply and therefore a deficit is experienced. The amount of water delivered by the pump is dependent on the solar intensity and hence the power delivered by the PV array according to the equation (40) above

It is noted that about 16% of the water requirement occurs outside the irradiation hours i.e. from sunset to sunrise. This significance is highlighted when it is also noted that the water delivered by the system during the day is 94% of the day water requirements by the maize crops.

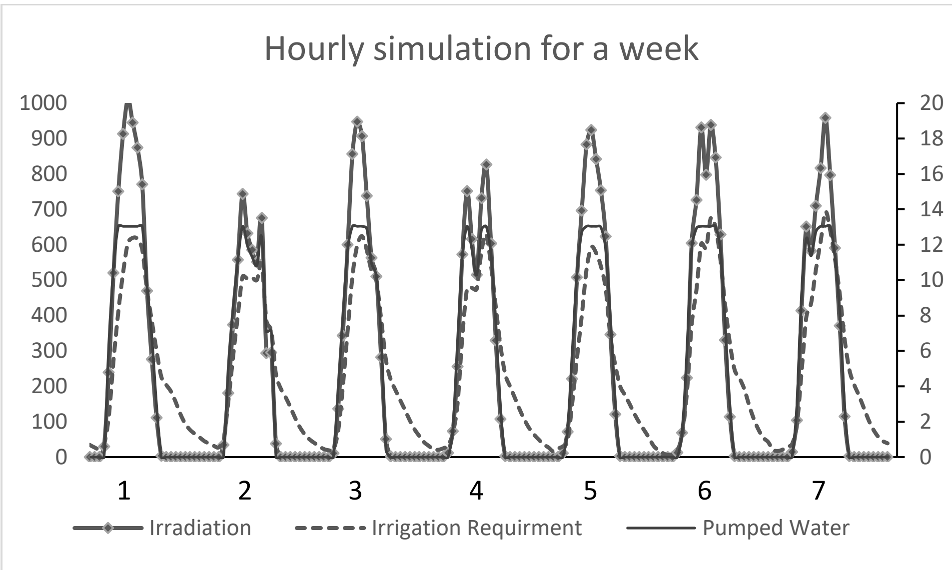

Figure 22: Hourly Simulation for a week

The pattern is the same for a simulation period of one week. The mismatches in the daily water balances occur during the night when there is no power supply to power the pump from the solar panels. It's also noted that almost in all the days, the water pumping is capped at 13 m^3/h which represents the maximum pumping capacity of the pump and coinciding with the period of maximum insolation of 1 kWh/m^2. The excess pumped water during the day compensates for the water demand during the night. This is enabled by use of the power controller that protects the pump from spoilage in cases of excess power input from the PV array.

The daily water balance yields another different scenario. As shown in Figure 23 below

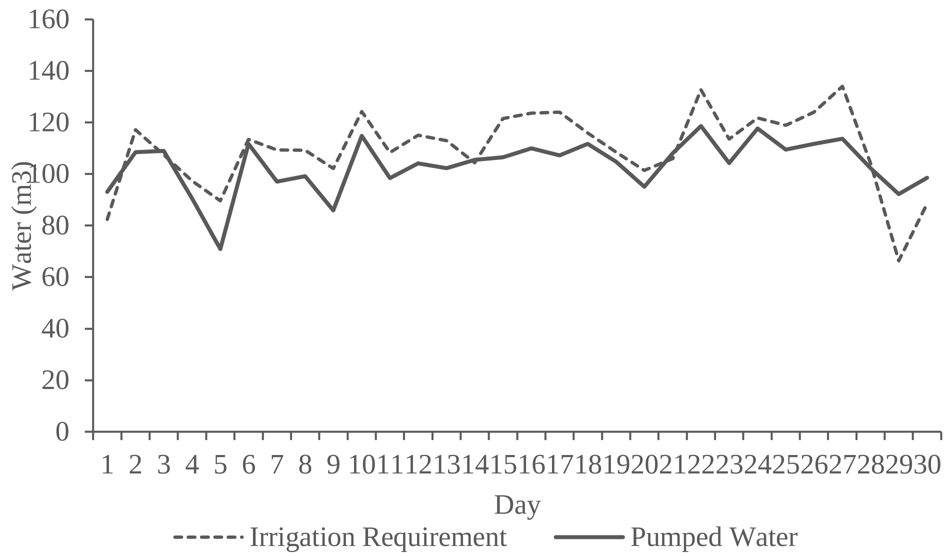

Figure 23: Daily Water Balance

It is observed that in almost all the days, the pumped water is less than the irrigation requirements by up to around 20%. This represents a significant amount. That explains an overall accumulation of about 8% deficit during the month.

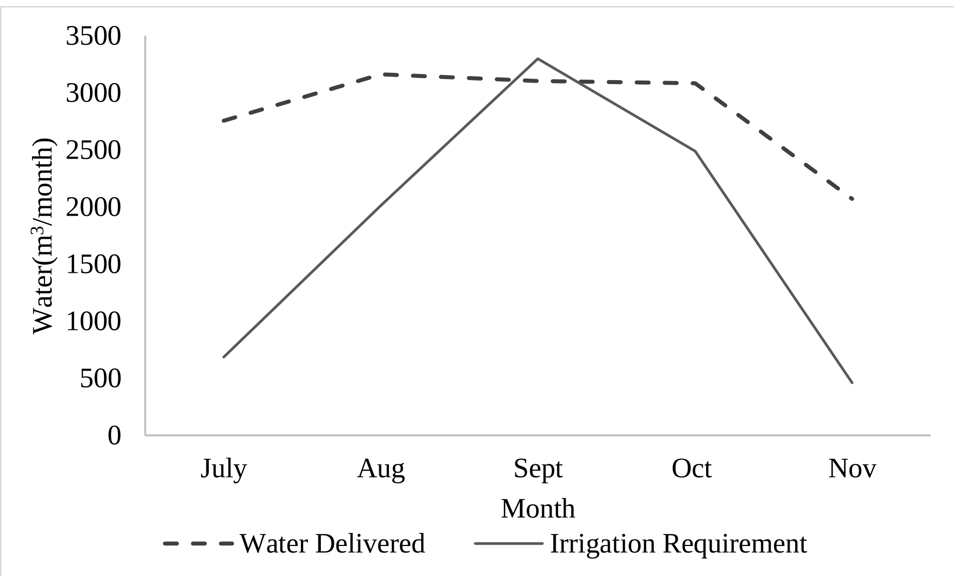

Figure 24: Monthly water balance

From Figure 24, the peak irrigation requirement is indeed in the month of September. It rises steadily from the planting date to September from which the demand falls gradually. From October, the demand falls sharply. The initial stage is marked by the crops having small leaf surface area exposed to the surroundings and as such, the rate of transpiration is low. This increases gradually as the crop develops to an optimum water requirement during the mid-season. Maize is harvested dry and when harvested with the lowest moisture content, the crop is left to dry out. In this late stage, the water requirement is approximately 25% of the peak water requirement. From this design, the lowest water requirement is in November which represents about 14% of the peak water requirement.

In the whole growth season, about 900mm of water is required in the field. In the same period, the system is able to pump 1400mm to the field. This represents an extra 56% water being unutilized. This is significant in an area that is grappling with water scarcity and harsh climatic conditions.

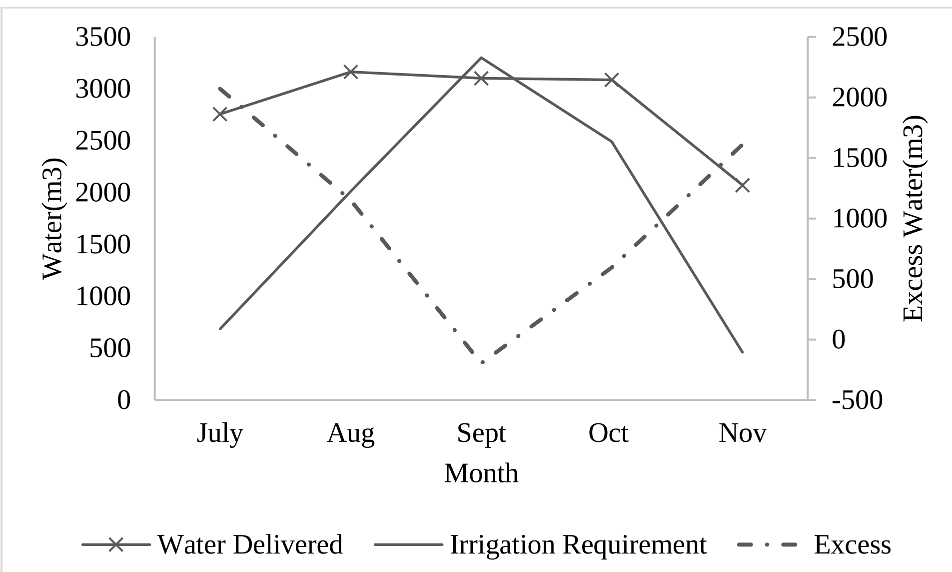

A deficit is experienced in the peak moth of September at about $200m^3$ while the other months experience excess water supply with the month of July receiving an excess of $2000m^3$.

From the analysis in Figure 1, it can be shown that the instantaneous weather variation has an effect on the effective performance of the SPIS. The design using the daily monthly averages was supposed to satisfy the water demand at the design month. As it turns out, however, the daily summations from the hourly simulations depict a difference. The discrepancies range from daily deficits of about 21 m^3 to surpluses of about 26 m^3 of water pumped. The deficits are created from the accumulation of water during the periods when there is no solar insolation i.e. at night.

The crop water requirements for the crop is about 890mm for the whole growing season. FAO guidelines put the water demand by maize at 500-900mm (FAO, 1998). The requirement is therefore higher. Considering this is a hot arid climate, the water requirement is highly influenced by higher temperatures and wind speeds, insolation and lower humidity and precipitation.

4.4 Economic Analysis

4.4.1 Crop Yield and Revenue

The simulation results from AquaCrop predicted the yield of the maize at 3 tons per hectare. Given the Kenya national average of 1.62 tons per hectare (USDA, 2017), this is more than double and presents a good prospect in increasing the productivity of agricultural lands which represent 80% of the country's land cover.

The climatic data used were the averages of rainfall, reference evapotranspiration and minimum and maximum daily average temperatures. Assuming no stress on the crop yield reduction was less than 2%. This crop production is strongly attributed to the drip irrigation system which ensures the water is available to the crop at the root of the crop hence eliminating weeds. This option is selected in the simulation process not to have weeds. Total biomass cover (dry weight) was predicted at 30 tons.

The fertilizer application rate guidelines provided by Kenya Agricultural Research Institute (KARI) (NAAIAP, 2014) provides fertilizer and top dressing rates of 200Kg/ha. This is to compensate for a deficiency in key mineral elements as potassium and ammonium.

The market prices of maize in Kenya due to the maize shortages emanating from drought experienced from late 2016 into 2017 is high. The average maize prices used by the national cereals and produce board (NCPB) was therefore used. It is however different for the different markets and towns.

Table 8: Maize Prices (July 2017) (AFA, 2017)

Town	Price in Ksh (for 90 Kg)
Nairobi	38
Mombasa	43
Loitoktok	30
Eldoret	43
Kisumu	48
Busia	31.5
Nakuru	32

An NCPB average of Ksh.40 (USD 0.4) per Kg was used in calculating the total revenue from the sale of maize grains. The biomass generated from the maize stalks would be sold as animal feed. However, to enrich the soil which is mildly deficient of organic matter, the maize stalks will be retained in the farm to form a source of organic matter and hence improve the productivity of the land in subsequent harvests.

4.4.2 Economic Analysis

The economic analysis of a system provides the means of comparison of one system to another in terms of affordability and profitability. Affordability comes from the initial investment costs that the investor has to incur before the system is fully functional. Profitability, on the other hand, considered the margin the investor would accrue from the project should he/she undergo the venture. This is determined by the revenue earned from the maize yield, the initial costs incurred, cost of farm inputs, farm operation costs, and the operation and maintenance costs.

The quotation for the prices was obtained from local distributors of pumping water solutions and irrigation systems yielded total initial costs including installation of USD 7565 for the PVWPS and USD 4413 for the DWPS. This includes the initial capital costs of the power system and the irrigation system. The costs comparison is indicated in Figure 25.

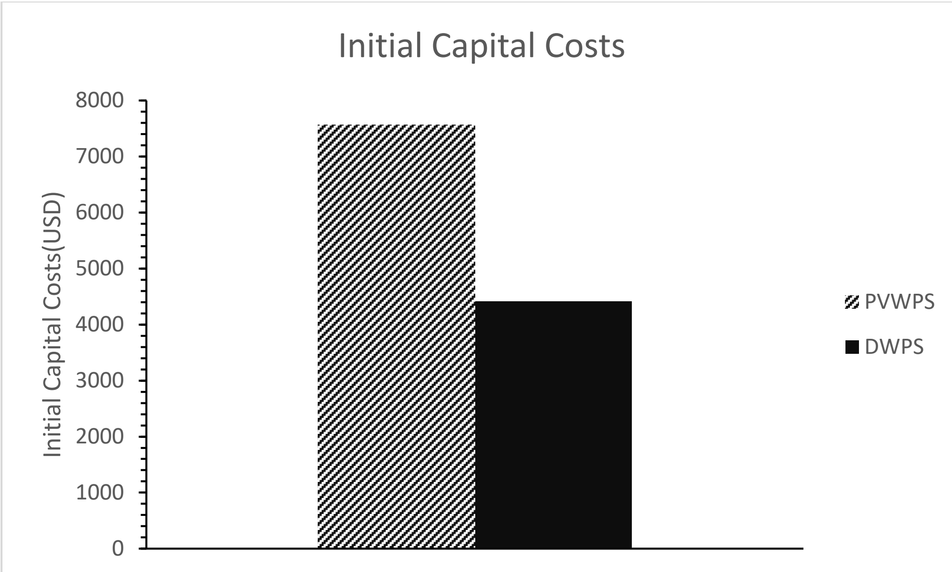

Figure 25: Total Initial Costs

From the graph, the total initial cost of the SWPS is over 40% more than the cost of the diesel-powered irrigation system. This is attributed to the cost of the power systems as all the other costs of the system remain the same. The initial cost is a factor that has been a problem to farmers especially small holder farmers who would want to venture into irrigation (FAO, 2015). The initial cost of the irrigation system represents USD 1.37/Wp for the SPIPS while it's about USD 1.1 per watt installed for the diesel water pumping system.

The high initial capital outlay of the solar powered irrigations system may be difficult for the farmers to invest into the system. Depending on access to capital, the farmer may opt to a system which they can afford to install. Coupled with the cost of the drip irrigation system which also has a significant value, cost and access to finance will play a critical role in its adoption.

A larger percentage of the initial costs is taken up by the cost of the energy supply system, i.e. the cost of solar PV array and the cost of diesel generator although the cost of PV modules has been reducing (IRENA, 2016b). The cost of PV panels has been reducing from the world market with a solar module in Kenya being retailed averagely at USD 0.59 /Wp.

From Figure 26, the cost of energy generation unit is about 43% in for the SWPS as compared to the DWPS at 23%. The SWPS, therefore, takes almost double the cost fraction of the initial costs in comparison. For the same output, the diesel generator costs USD 1178 compared to the solar array valued at USD 3,480. The government of Kenya gazette by the energy regulations commission (ERC) shelved value added tax (VAT) and zero-rated import duty on solar PV panels and accessories (ERC, 2012). It has however given a competitive challenge to solar PV manufacturing firms in the country with such as Solinc East Africa being the first in the country to take the initiative (Solinc, 2016). This in effect has reduced the initial cost of PV system, though still higher than diesel generator prices which surprisingly receives a tax exemption despite its huge carbon footprint.

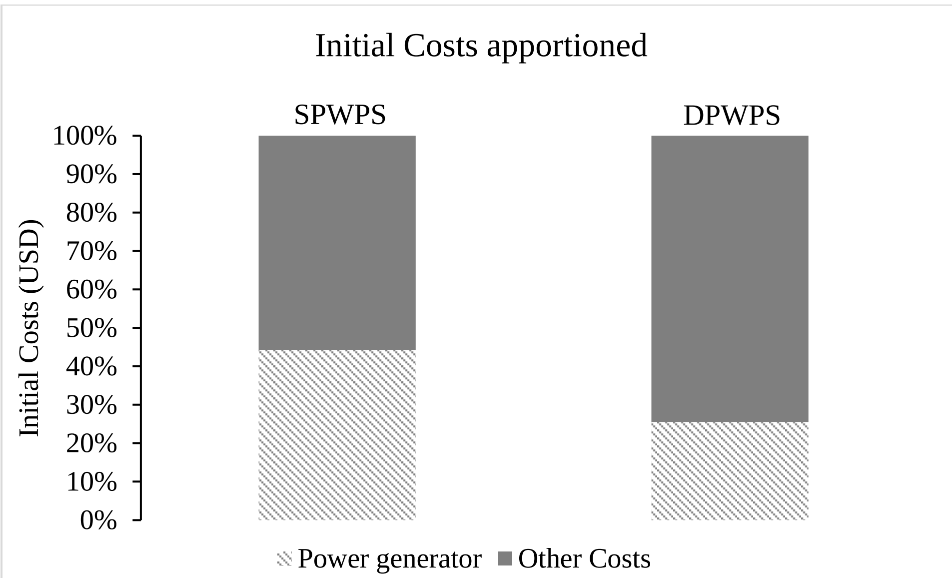

Figure 26: Cost of Energy generation system

Operation and maintenance costs

4.4.3 Fuel Prices

The fuel consumption of the generator is indicated at 295g per kWh of power produced with a tank capacity of 15 litres. Using the total power requirement of 8900 m^3 of water used per irrigation season by the crop, the energy requirement is given as

$$\frac{1000 \times 9.81 \times 40 \times 8900}{3600 \times 1000} = 970.1\ Kwh\ per\ irrigtion\ season$$

Therefore, the fuel requirement=fuel consumption rate*power requirement/Density of fuel

Fuel consumption per growing season= $970.1(\ kwh) \times \frac{295\left(\frac{g}{kwh}\right)}{832\left(\frac{g}{l}\right)}$ =344 litres

The cost of fuel per growing season is calculated=$price\ of\ fuel \times quantity\ of\ fuel$

$$= 0.9\ (\frac{USD}{l})\ \times 344$$

$$= USD\ 309.6$$

$$and\ for\ two\ growing\ seasons\ in\ a\ year = USD\ 619$$

This was used as the annual fuel costs for the two seasons annually.

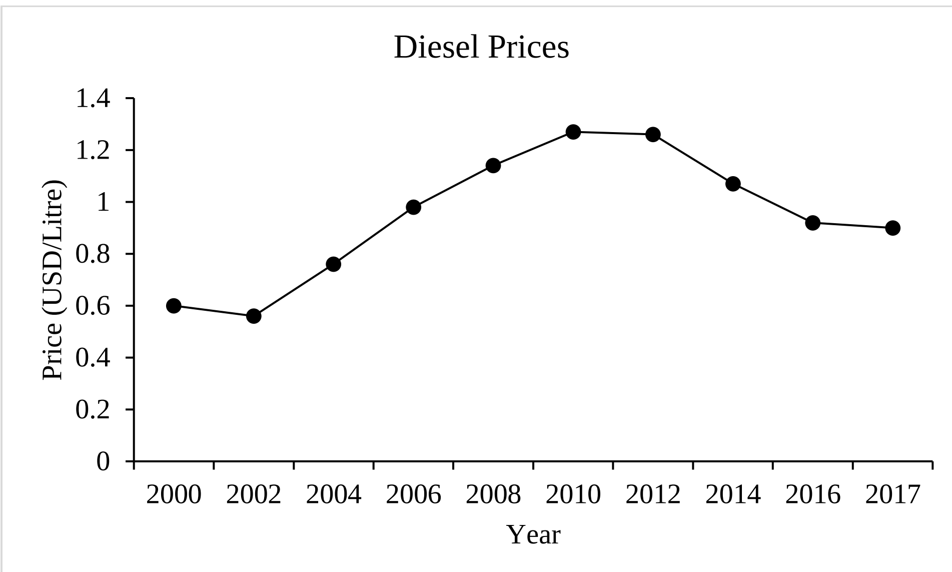

Figure 27: Fuel Pump Prices

Diesel prices in Kenya have been averagely increasing since 2002. Despite the fall in global fuel prices, its benefits are yet to be realized by the consumers. The pump prices of diesel have increased gradually from a low of about USD 0.56 in 2002 to an all-time high of USD 1.27 in 2010. Price regulations are being regulated by the energy regulatory commission (ERC). The government has, in essence, increased the levies on fuel making the gains of the falling in crude oil prices not to be felt.

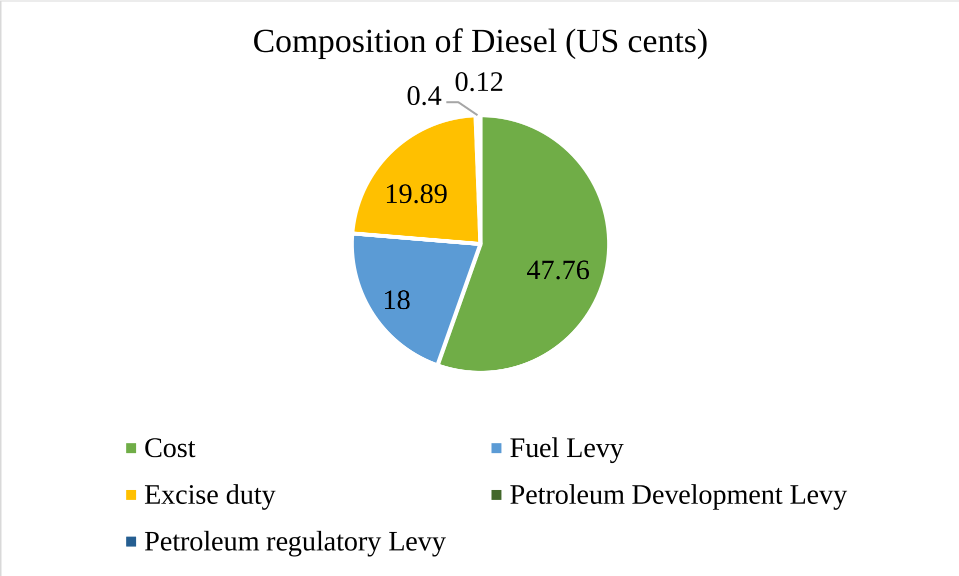

Figure 28: Diesel Fuel Charges

Over 44% of the pump prices of fuel is taken up by levies and taxes. Excise duty and fuel levy take the largest chunk of the taxation accounting for over 98% (Munda, 2016). The price of fuel, which is the main operation cost for diesel pumping system increases the life cycle cost of the diesel water pumping system.

In addition to the cost of fuel, the DWPS is associated with the cost of replacement of filters, lubrication oils, oil rings, piston rings etc. and the periodic servicing after the indicated running hours of the diesel generator. The price of fuel is expected to increase due to the predicted scarcity of fossil fuels (Twidell & Weir, n.d.). In addition, as the diesel generator cumulative operating hours increases, the frequency of maintenance costs increase due to wear and tear.

The SWPS has low maintenance costs mostly related to the cleaning of the surface of the panels to get rid of dust. The place having less vegetation during the no rain period leaves the soil prone to being blown and deposited on the surface of the panels. The dust deposits create a hard-shading effect reducing the amount of solar irradiation reaching the solar panels hence reducing its production capacity. Partial shading has the effect of reducing the voltage output of the PV array (Reza et al., 2016). Mejia et al. (Mejia, Kleissl, & Bosch, 2014) registered losses up to 0.21% per day. Less maintenance and operation cost is, therefore, the advantage that SWPS have over the DWPS.

4.4.4 Profitability

A farmer's interest in investing in an irrigation system is to increase its productivity and hence his profit margin. The profitability of this project was assessed through the use of the net present value (NPV), payback time and the internal rate of return. A discounting rate of 10% was used in the assessment.

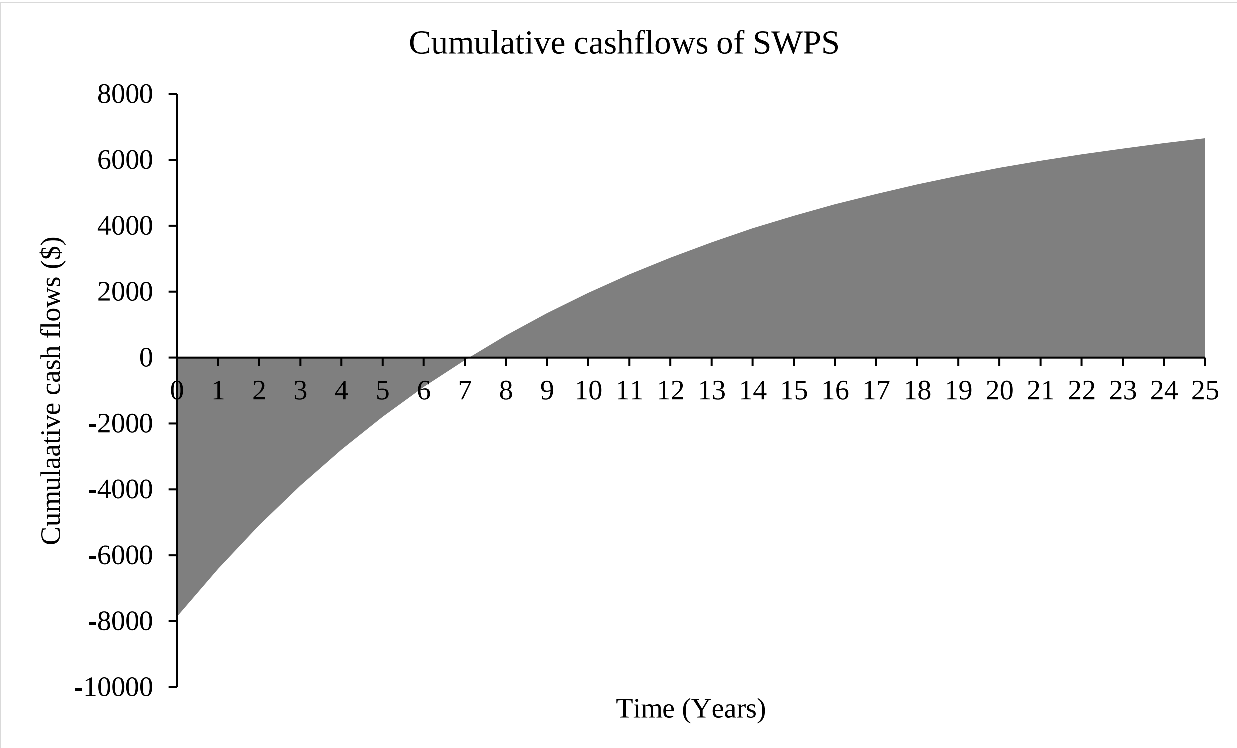

Figure 29: Cumulative cashflow of SWPS

Figure 29 shows the cumulative discounted cashflow, which in essence represents the net present value of the project at the year indicated if the project life was equal to that year. Both power systems were taken to have a project life of 25 years. Year 0 represents the initial time of the project when the investment has just been made.

When revenues from maize sales from the first year are realized, the costs incurred in the investment start to be recouped. The payback time of the SWPS, the time when the project breaks even is 7 years.

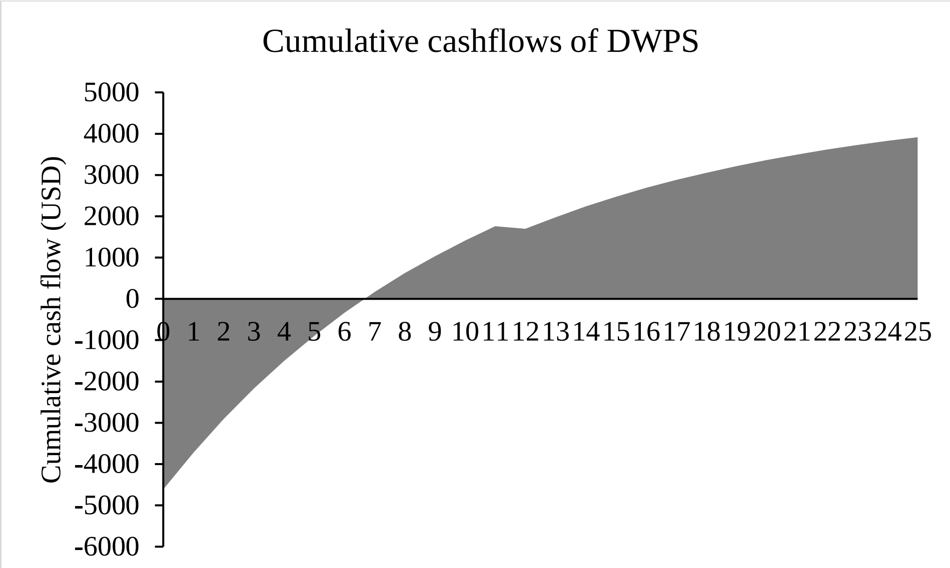

Figure 30: Cumulative cashflows of DWPS

The payback time for the diesel-powered irrigation system is 6.67 years i.e. 6 years 8 months. The DWPS, therefore, recoups the investment earlier than the SPWPS albeit by just 4 months. Given the higher initial costs of the SPWPS than the DWPS and serving the same water demand, the recoupment rate is higher in the former. Depending on the quality of the diesel generator engine, replacement of the whole engine or the whole generator may be necessitated after a certain period e.g. 10-12 years. This is indicated in the 11-12th year by a reduction in the cumulative cashflows.

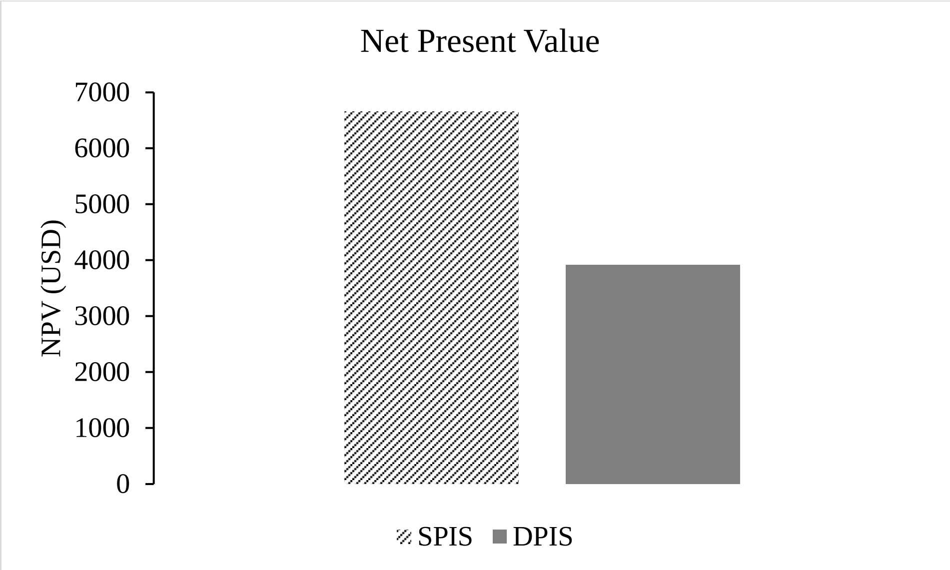

Figure 31: NPV comparison of SPIS and DPIS

Both projects give a positive net present value indicating they are profitable to invest in. The NPV is higher in SPIS than in DPIS at USD 6,658 and USD 3,914 respectively representing a 41% higher profitability of the SPIS. In the current era where the price of PV products has become lower coupled with the government of Kenya policies to bolster development of renewable energy products, the profitability is to be considered in good light. It would be a platform for solar development companies, policy makers and development partners to pitch to farmers. It would thus be wiser for farmers to invest in SPIS.

To ascertain their level of profitability, the internal rate of return for the two systems were determined. IRR helps in comparison of the projects and comparing with the cost of finance. The DPIS has an IRR of 21.08% while the SPIS has a return of 20.5%. The IRR represents the return on capital invested in the project per year. From these two systems, therefore it indicates that the two systems are almost at par but SPIS has a higher internal return on investment.

4.4.5 Cost and Source of Financing

Kenya introduced a cap on lending rates at a maximum of 4.5% above the central bank of Kenya (CBK) base lending rate of 10% meaning banks can lend to clients at a maximum interest rate of 14.5%. According to the CBK, the weighted average lending rates of banks since the capping of interest rates in September 2016 to June 2017 was 13.61% (CBK, 2017). The IRR of both irrigation systems is higher than the cost of acquiring finance implying that even though the banks charged the maximum lending rate, the ventures would still make profits. Agricultural finance corporation (AFC), a government institution set up by the government to lend to farmers at affordable interest rates with collateral. This further appraises the investments.

The economic indicators are summarized in Table 9

Table 9: Economic analysis summary

Economic Indicators	**SPIS**	**DPIS**
Initial Costs (USD)	7,565	4,413
Net Present Value (USD)	6,658	3,914
Payback Time (years)	7	6.67
Internal Rate of Return (USD)	21.08	20.5

CHAPTER 5: DISCUSSION AND CONCLUSION

The main purpose of this study has been to design a system and develop a dynamic model that would be used to simulate and optimize the standalone water pumping and irrigation system in order to assess the feasibility of solar water pumping for use in irrigating agricultural crops in hot arid climates. This has been done by assessing the solar intensity and the irrigation water requirement and the performance of the system under the conditions to satisfy the IWR.

5.1 Effect of environmental variability in performance of the SPIS

Both solar intensity and IWR are affected by weather conditions hence the performance of the designed system. The effectiveness of the SPIS in meeting the water demand depends on the solar intensity and the performance of the solar arrays. High temperatures reduced the efficiency of the PV arrays while increasing the irrigation water requirement. It was also seen that the solar insolation provided almost a replica change on the IWR and is seen to have the highest impact on its change together with the wind. The highest stress is realized when the weather conditions combine to reduce the performance and production of the solar arrays while also increasing the irrigation water requirement.

The irrigation water requirements in Saretho, Garissa, which is a hot arid climate is high. Higher water demand is particularly highest in the mid-season stage when the crop is in development. This should be paramount in planting to reduce the IWR. The timing of planting season should be in such a way that the mid-season stage coincides with the peak rainy season or month in order to reduce the peak water demand from irrigation. Although the IWR is higher, it should be considered that the system would have required a bigger system were it not for the water saving technology. The high irrigation and application efficiency of the drip irrigation system lowered the demand to pump more water. In these conditions, therefore water saving technologies should be used to save the water requirement.

The area being a hot climate had an effect of reducing the performance of the PV panels and their productivity. This has the effect of reducing the water delivered by the SPIS. Increased reduction of in efficiencies of the solar arrays is particularly important during peak solar intensities during the day not only because of the peak hourly demand during mid-day but also the significance of the peak solar intensity at that time. At high solar intensities, the IWR is highest while the temperatures are relatively higher with the effect that it reduces the efficiency of the solar array.

During the other growing stages, the capacity of the system exceeds the water demand by the crops. It should be noted that the design month is the only time when the demand and supply match. Other months experience periods in which the supply is greater. Coupled with a distribution system, the excess water delivered could be used for providing drinking water to the cattle. The community is a pastoralist community and providing water for the animals would reduce their movement in search of it. Efforts should be made also to have short term crops be incorporated by expanding the area under cultivation. Vegetables and fodder is an alternative. For other areas, uses could be devised for use of the excess water supply. A consideration is also made that this is a remote area with no grid extension. Electricity supply to the resident household is limited and the primary reason for the use of the energy system instead of the grid. The use of the excess power would also be used for the supply of electricity to the households. Given that some countries have introduced feed-in tariffs/net metering in their national policy, excess power connection to the national grid is a possibility.

The directly coupled system matches quite well with an irrigation system. With large dependence on irradiation, crop water demand is met with the system albeit daily cumulative totals due to mismatches associated with night evapotranspiration. The crop water requirements match well with the solar intensity during the day providing enough power to suffice the hourly demand during the day. Soil retention capability might play an important role for this system since excess supply is experienced during the irradiation hours and a small deficit during the night hours. The small demand during the night doesn't warrant a battery system since it is within 4% of the total daily demand.

5.2 Techno-Economic feasibility of SPIS in comparison with DPIS

The initial costs associated with SPIS are high despite the reducing price of the solar PV arrays. This is particularly important in arid climates which have been exhibited to have higher irrigation requirement than cool humid climates necessitating larger arrays. It is, however, able to return higher rates of investments as compared to the DPIS. Cost of finance and source of funding is critical in the dissemination of SPIS. The profitability and attractiveness to small holder farmers to adopt the technology anchors on their access to low cost funding. This is because of the initial capital outlay involved in acquiring the energy system.

DPIS, on the other hand, exhibits low initial costs but also lower returns for the same acreage. Its higher maintenance and operation cost lowers its profitability. Fuel, taking the main chunk of the operation costs, drives the economic viability of DPIS. The prices of fuel will have to remain constant or dip for it to remain competitive with SPIS. Although the global fuel prices have been on a downward spiral they seem to have reached the base and are on the upward spiral. With remote communities being far away from the pipeline termini, the prices in these areas are higher than in urban centres due to transportation charges.

Irrigation systems have the potential to increase the productivities of the areas under cultivation. The study revealed an increase in productivity yielding higher than the normal country averages. Hot arid climates suffer from water scarcities and low rainfall. Increasing productivity goes a long way to alleviate food scarcity associated with these areas. The average production from arid and semi-arid areas is quite low. In sub-Saharan countries where the irrigation potential is still huge and the climatic conditions becoming harsh, expanding arid areas seems to be a logical step in meeting the Millennium Development goal on food security.

5.3 Limitation of the study

While conducting the economic analysis, the lifetime of the project was taken as 25 years. The result might apply for the price of the components and revenue collected but the irrigation water requirement is dependent on the climatic conditions during the project life. Climate changes during this duration would have an effect on the performance of the system to sustain demand.

The irradiation data used were the values which took into account the actual weather conditions during the year and not the clear sky model data. It is therefore assumed that cloud cover during the period is catered for. There was, therefore, no need to include days in which the area would possibly be under cloud cover for the days under consideration.

5.4 Conclusion

The study was able to come up with a design and simulation of irrigation load and performance of the overall system in meeting the demand. It was deduced that the preliminary design did meet the instantaneous hourly loads during the peak month on some hours and cumulatively on some hours. Mismatches in the system were present during other growth stages of the plant. From the analysis, it was determined that:

The weather conditions had various effects on the load as well as the performance of the PV. The optimal sizing is highly dependent on good prediction of the weather condition that determines the crop water requirement and solar intensity. The irradiation and weather condition are thus critical in developing a good solar powered irrigation system.

The SPIS is more economical in almost all aspects but for the initial costs and the payback time than the DPIS. Further reduction in array prices is deduced to be the main factor to drive the profitability of SPIS and reduce its initial capital costs.

Solar powered irrigation system for irrigation of maize is technically and economically feasible for use in hot arid areas.

5.5 Recommendations

5.5.1 Recommendations for further research

The irrigation water requirement is dependent on the climatic conditions of the specific place. Climate change has the effect of providing a variation in the weather conditions, the main determinants of the crop water requirements. Global warming, for instance, raises the average climatic conditions per year, while climate change agreements and implementation tend to lower their rise. A study should, therefore, be carried out that incorporates the predicted environmental conditions during the lifetime of the projects and accompanying change in crop water demand. This will refine the results in respect to system stability for future scenarios. Climate agreements also have the impact of imposing penalties or additional rebates on carbon footprint prices. A study that incorporates these would help in providing a roadmap for future investments.

The effect of wind in cooling the PV panels in areas where the wind speeds are high shouldn’t be ignored. Low temperatures have been known to increase the performance of the PV modules. Further research needs to be carried out to incorporate the cooling effect of wind on the PV modules performance viz a viz the overall performance of the system.

5.5.2 Recommendations to the investors and policy makers

The SPIS are economically viable provided low cost of financing available so as not to erode the gains made in the reducing cost of PV modules. The arid areas which often have low land rates would provide a good investment opportunity. Although the sizes of the stems are larger to carter for the higher demands during periods of high stress, the productivity is commensurate.

Policies to reduce taxation and import duties on PV modules will reduce the initial cost associated with SPIS. It is therefore inherent on the governments to develop an initiative that will reduce the initial costs of PV modules. The Kenyan government has taken the initiative to zero rate the PV modules despite the lower cost of electricity associated with hydro and geothermal sources respectively. Increasing subsidies associated with the manufacture of the modules might spur local manufacturers like Solinc East Africa

5.5.3 Recommendations to the Institute

Carrying out meaningful research requires funding. Some software is expensive for the students to purchase while still supporting themselves in the research centres. It would be prudent for the administration to source and introduce research funding as it constitutes constraints to the work to be done by the researchers in trying to carry out the objectives of the research.

REFERENCES

Abdul-wahid, S. N., & Judh, A. H. (2009). Calculation of Linke turbidity in atmosphere over Iraq by solar constant. In *2nd Conference of Pure and Applied Sicences* (Vol. 1). Iraqi Academic Scientific Journals.

Abouzahr, I., & Ramakumar, R. (1991). Loss of Power Supply Probability of stand-alone Photovoltaic Systems: A Closed Form Approach. *IEE*, *6*(1).

AFA. (2017). Maize prices. Retrieved July 22, 2017, from http://www.agricultureauthority.go.ke/dry-maize-per-bag-nairobi-ksh-3800-mombasa-ksh-4300-kisumu-ksh-4800-nakuru-ksh-3200-eldoret-ksh-4300-loitoktok-ksh-3000-busia-ksh-3150/#

Ahmad, G. E. (2002). Photovoltaic-powered rural zone family house in Egypt. *Renewable Energy*, *26*, 379–390.

Aljazeera. (2017). Number of Kenyans going hungry doubles to three million. Retrieved May 12, 2017, from http://www.aljazeera.com/news/2017/03/number-kenyans-hungry-doubles-3-million-170328110811329.html

Allen, R. G., Pereira, L. S., Raes, D., & Smith, M. (1998). Allen_FAO1998, 1–15.

Alsayed, M., Cacciato, M., Scarcella, G., & Scelba, G. (2013). Multicriteria Optimal Sizing of Photovoltaic-Wind Turbine Grid Connected Systems. *Transaction on Energy Conversion*, 1–10. http://doi.org/10.1109/TEC.2013.2245669

Alushula, P. (2017). Bura irrigation scheme to retire expensive diesel pump system. Retrieved May 12, 2017, from https://www.standardmedia.co.ke/business/article/2000230688/bura-irrigation-scheme-to-retire-expensive-diesel-pump-system

Anis, W. R., & Metwally, H. M. B. (1994). Dynamic performance of a directly coupled PV pumping system. *Solar Energy*, *53*(4), 369–377. http://doi.org/10.1016/0038-092X(94)90040-X

Arab, A. H., Driss, B. A. I. T., Amimeur, R., & Lorenzo, E. (1995). Photovoltaic Systems Sizing for Algeria. *Solar Energy*, *54*(2), 99–104. http://doi.org/doi.org/10.1016/0038-092X(94)00091-Q

Basso, B., Cammarano, D., & Carfagna, E. (2013). Review of Crop Yield Forecasting Methods and Early Warning Systems. *FAO*, 1–56.

Bhuiyan, M. M. H., & Asgar, M. A. (2003). Sizing of a stand-alone photovoltaic power system at Dhaka. *Renewable Energy*, *28*, 929–938.

Brand, B., & Missauoui, R. (2014). Multi-Criteria analysis of electricity generation mix scenarios in Tunisia. *Renewable and Sustainable Energy Reviews*, *39*, 251–261. http://doi.org/10.1016/j.rser.2014.07.069

Brown, P. (2014). *Basics of Evaporation and Evapotranspiration*. Arizona.

Campana, P. E. (2015). *PV water pumping systems for agricultural applications*.

Campana, P. E., Li, H., & Yan, J. (2013). Dynamic modelling of a PV pumping system with special consideration on water demand. *Applied Energy*, *112*, 635–645. http://doi.org/10.1016/j.apenergy.2012.12.073

CBK. (2017). Interest rates. Retrieved July 22, 2017, from https://www.centralbank.go.ke/statistics/interest-rates/

Celik, A. N. (2003). Techno-economic analysis of autonomous PV-wind hybrid energy systems using different sizing methods. *Energy Conversion and Management*, *44*, 1951–1968. http://doi.org/10.1016/S0196-8904(02)00223-6

Chand, V., & Kalamkar, V. R. (2016). Solar photovoltaic water pumping system - A comprehensive review. *Renewable and Sustainable Energy Reviews, 59*, 1038–1067. http://doi.org/10.1016/j.rser.2016.01.021

Chandel, S. S., Nagaraju Naik, M., & Chandel, R. (2015). Review of solar photovoltaic water pumping system technology for irrigation and community drinking water supplies.

Renewable and Sustainable Energy Reviews, *49*, 1084–1099. http://doi.org/10.1016/j.rser.2015.04.083

Chel, A., Tiwari, G. N., & Chandra, A. (2009). Simplified method of sizing and life cycle cost assessment of building integrated photovoltaic system. *Energy and Buildings*, *41*, 1172–1180. http://doi.org/10.1016/j.enbuild.2009.06.004

Daze, A. (2012). *Adaptation Learning Programme (ALP) Climate Change Vulnerability and Adaptive Capacity in Garissa County , Kenya*. Nairobi.

Dongue, S. B., Njomo, D., & Ebengai, L. (2013). An Improved Nonlinear Five-Point Model for Photovoltaic Modules. *International Journal of Photoenergy*, *2013*(iii). http://doi.org/10.1155/2013/680213

Dubey, S., Sarvaiya, J. N., & Seshadri, B. (2013). Temperature Dependent Photovoltaic (PV) Efficiency and Its Effect on PV Production in the World A Review. *Energy Procedia*, *33*, 311–321. http://doi.org/10.1016/j.egypro.2013.05.072

Đurin, B., & Baić, L. (2016). The Method of Selecting the Optimal Variant of Irrigation Systems Driven by PV Energy. *American Scientific Research Journal for Engineering, Technology, and Sciences (ASRJETS)*, *27*(1), 225–243.

ERC. (2012). Solar Energy. Retrieved July 22, 2017, from http://www.renewableenergy.go.ke/index.php/content/31

Fanney, A. H., Davis, M. W., Dougherty, B. P., King, D. L., Boyson, W. E., & Kratochvil, J. A. (2006). Comparison of Photovoltaic Module Performance Measurements. *Solar Energy Engineering*, *128*(May). http://doi.org/10.1115/1.2192559

FAO. (1998). Single crop Coefficient. Retrieved from http://www.fao.org/docrep/X0490E/x0490e0b.htm#crop coefficients

FAO. (2015). Prospects for solar-powered irrigation systems (SPIS) in developing countries, (May), 1–19. http://doi.org/http://www.royalcommission.vic.gov.au/finaldocuments/summary/PF/VBRC_

Summary_PF.pdf

FAO. (2016). Introduction to AquaCrop. Retrieved from http://www.fao.org/documents/card/en/c/ba35b63c-596a-467d-95fe-dfcfca6da2a9/

FAO. (2017). Kenya subsidises maize imports. Retrieved May 12, 2017, from http://www.fao.org/giews/food-prices/food-policies/detail/en/c/886937/

Firmanda, D., Riza, A., & Gilani, S. I. H. (2014). Standalone Photovoltaic System Sizing using Peak Sun Hour Method and Evaluation by TRNSYS Simulation. *International Journal of Renewable Energy*, *4*(1), 1–6.

Ganesan, T., Vasabt, P., & Elamvazuthi, I. (2017). Multiobjective Optimization of Solar Powered Irrigation System with Fuzzy Type-2 Noise Modelling.

Garni, H. Al, Kassem, A., Awasthi, A., Komljenovic, D., & Al-haddad, K. (2016). A multicriteria decision making approach for evaluating renewable power generation sources in Saudi Arabia. *Sustainable Energy Technologies and Assessments*, *16*, 137–150. http://doi.org/10.1016/j.seta.2016.05.006

Gelaro, R., McCarty, W., Suarez, M. j., Todling, R., Molod, A., Takacs, L., … Zhao, B. (2017). The Modern-Era Retrospective Analysis for Research and Applications Version 2 (MERRA-2). *Journal of Climate*, *2*. http://doi.org/10.1175/JCLI-D-16-0758.1

Ghoneim, A. A. (2006). Design optimization of photovoltaic powered water pumping systems. *Energy Conversion and Management*, *47*, 1449–1463. http://doi.org/10.1016/j.enconman.2005.08.015

Glasnovic, Z., & Margeta, J. (2007a). A model for optimal sizing of photovoltaic irrigation water pumping systems. *Solar Energy*, *81*, 904–916. http://doi.org/10.1016/j.solener.2006.11.003

Glasnovic, Z., & Margeta, J. (2007b). Optimization of Irrigation with Photovoltaic Pumping System, 1277–1297. http://doi.org/10.1007/s11269-006-9081-8

GoK. (2015). *Climate Risk Profile Garissa County*. Nairobi.

Gokmen, N., Hu, W., Hou, P., Chen, Z., Sera, D., & Spataru, S. (2016). Investigation of wind speed cooling effect on PV panels in windy locations. *Renewable Energy*, *90*, 283–290. http://doi.org/10.1016/j.renene.2016.01.017

Goletsis, Y., Psarras, J., & Samouildis, J.-E. (2003). Project Ranking in the Armenian Energy Sector Using a Multicriteria Method for Groups. *Annals of Operations Research*, *120*, 135–157. http://doi.org/dx.doi.org/10.1023/A:1023330530111

Gommes, R. (1998). Crop-Yield Weather Modelling. In *FAO-WMO Roving Seminar*.

Gordon, J. M. (1987). Optimal sizing of stand-alone photovoltaic solar power systems. *Solar Cells*, *20*, 295–313. http://doi.org/doi.org/10.1016/0379-6787(87)90005-6

Haddad, S., Benghanem, M., Mellit, A., & Daffallah, K. O. (2015). ANNs-based modeling and prediction of hourly fl ow rate of a photovoltaic water pumping system : Experimental validation. *Renewable and Sustainable Energy Reviews*, *43*, 635–643. http://doi.org/10.1016/j.rser.2014.11.083

Hasan, A., Mccormack, S. J., Huang, M. J., & Norton, B. (2014). Energy and Cost Saving of a Photovoltaic-Phase Change Materials (PV-PCM) System through Temperature Regulation and Performance Enhancement of Photovoltaics. *Energies*, *7*, 1318–1331. http://doi.org/10.3390/en7031318

Hee Yau, P. (2006). *Generation System Reliability Evaluations with Intermittent Renewables*. University of Strathclyde.

Hellman, H., Koivisto, M., & Lehtonen, M. (2014). Photovoltaic Power Generation Hourly Modelling. In *Proceedings of the 2014 15th International Scientific Conference on Electric Power Engineering*. Brno: IEEE. http://doi.org/10.1109/EPE.2014.6839426

Hille, G., & Franz, M. (2011). *Grid Connection of Solar PV Technical and Economical Assessment of Net-Metering in Kenya Authors*. Berlin.

Hosseinin, S. H., Ghaderi, S. F., & Shakouri, G. H. (2012). An Investigation on the Main Influencing Dynamics in Renewable Energy Development-A Systems Approach. In *Second*

Iranian Conference on Renewable Enenergy and Distributed Generation (pp. 92–97). Tehran: IEEE. http://doi.org/10.1109/ICREDG.2012.6190476

IREK. (n.d.). *A desk assessment on the overviews of current solar and wind energy projects in Kenya*. Eldoret.

IRENA. (2016a). *Solar pumping for irrigation : Improving livelihoods and sustainability*. Abu Dhabi.

IRENA. (2016b). *Solar PV in Africa:Costs and Markets*. Bonn: International Renewable Energy Agency.

Irmak, S., Odhiambo, L. O., Kranz, W. L., & Eisenhauer, D. E. (2011). Irrigation Efficiency and Uniformity , and Crop Water Use Efficiency Irrigation Efficiency and Uniformity , and Crop Water Use Efficiency. *Biological Systems Engineering*. Retrieved from http://digitalcommons.unl.edu/biosysengfacpub/451

IWMI. (2010). *Managing Water for rainfed agriculture*. *Water Issue Brief*. Colombo.

Jakhrani, A. Q., Othman, A.-K., Rigit, A. R. H., Samo, S. R., & Kamboh, S. A. (2012). Life Cycle Cost Analysis of a Standalone PV System. In *2012 International Conference in Green nd Ubiquitous Technology* (pp. 1–4). Jarkata: IEEE.

Kalogirou, S. A., & Arzu, Ş. (2010). Artificial Intelligence Techniques in Solar Energy Applications. In D. R. Manyala (Ed.), *Solar Collectors and Panels,Theory and Applications* (p. 15-). Shanghai: Sciyo. Retrieved from http://www.intechopen.com/books/solar-collectors-and-panels--theory-and- applications/artificial-intelligence-techniques-in-solar-energy-applications%0AInTech

Karina, F. Z., & Mwaniki, A. W. (2011). *Irrigation Agriculture in Kenya*. Nairobi.

Kaushika, N. D. Ã., & Rai, A. K. (2006). Solar PV design aid expert system. *Solar Energy Materials and Solar Cells*, *90*, 2829–2845. http://doi.org/10.1016/j.solmat.2006.04.010

Kazem, H. A., Khatib, T., & Sopian, K. (2013). Sizing of a standalone photovoltaic / battery system at minimum cost for remote housing electrification in Sohar , Oman. *Energy & Buildings*, *61*, 108–115. http://doi.org/10.1016/j.enbuild.2013.02.011

Kazem, H. A., Miqdam, A. H. A. A., Chaichan, M. T., Al-Mamari, A. S., & Al-Kabi, A. H. (2016). Design , measurement and evaluation of photovoltaic pumping system for rural areas in Oman. *Environment, Development and Sustainability*. http://doi.org/10.1007/s10668-016-9773-z

Kenna, J., & Gillet, B. (1985). *A handbook of Solar Water Pumping*. Southampton,London: Intermediate Technology Publications.

Khatib, T. (2010). Design of PV Water Pumping System at Minimum Cost for Palestine: A review. *Journal of Applied Sciences*.

Khatib, T., Ibrahim, I. A., & Mohamed, A. (2016). A review on sizing methodologies of photovoltaic array and storage battery in a standalone photovoltaic system. *ENERGY CONVERSION AND MANAGEMENT*, *120*, 430–448. http://doi.org/10.1016/j.enconman.2016.05.011

Khatib, T., Mohamed, A., & Sopian, K. (2013). A review of photovoltaic systems size optimization techniques. *Renewable and Sustainable Energy Reviews*, *22*, 454–465. http://doi.org/10.1016/j.rser.2013.02.023

Levidow, L., Zaccaria, D., Maia, R., Vivas, E., Todorovic, M., & Scardigno, A. (2014). Improving water-efficient irrigation : Prospects and difficulties of innovative practices. *Agricultural Water Management*, *146*, 84–94. http://doi.org/10.1016/j.agwat.2014.07.012

Malek, E. (1992). Night-time evapotranspiration vs . daytime and 24 h evapotranspiration. *Journal of Hydrology*, *138*, 119–129.

Mejia, F., Kleissl, J., & Bosch, J. L. (2014). The effect of dust on solar photovoltaic systems. *Energy Procedia*, *49*, 2370–2376. http://doi.org/10.1016/j.egypro.2014.03.251

Mellit, A. (2006). Artificial intelligence based-modeling for sizing of a Stand-Alone Photovoltaic Power System : Proposition for a New Model using Neuro-Fuzzy System(ANFIS). In *2006,* *3rd International Conference Intelligence systems* (pp. 606–611). IEEE. http://doi.org/10.1109/IS.2006.348488

Mellit, A. (2008). International Journal of Sustainable Sizing of stand-alone photovoltaic power supply system based on genetic algorithm and neuro-fuzzy : application for isolated areas. *International Journal of Sustainable Energy*, (July 2014), 49–60. http://doi.org/10.1080/14786450802264265

Mermoud, A. (2004). Pumping system sizing and modelling tool. In *19th European Photovoltaic Solar Energy Conference and Exhibition* (pp. 3–6).

Michaelowa, A., Kohler, M., Friedmann, V., Drasfield, B., & Tkacik, J. (2016). *Case Study: Health,Wealth and Solar Irrigation in In Kenya*. Viena.

MINES. (2017). HelioClim-3 Archives. Retrieved June 16, 2017, from http://www.soda-pro.com/web-services/radiation

Mude, A., Ouma, R., Van de Steeg, J., Kariuki, J., Opiyo, D., & Tipilda, A. (2007). *Kenya Adaptation to Climate Change in the Arid Lands: Anticipating, Adapting to and Coping with Climate Risks in Kenya - Operational Recommendations for KACCAL*. Nairobi,Kenya.

Munda, C. (2016, July 14). Why fuel prices shot up, Governemnt collects Sh38 levies, taxes per litre of petrol. *The Star*. Naiarobi. Retrieved from http://www.the-star.co.ke/news/2016/07/14/why-fuel-prices-shot-up-governemnt-collects-sh38-levies-taxes-per_c1385534

NAAIAP. (2014). *Soil Suitability Evaluation for Maize Production in Kenya*. Nairobi.

Narvate, L., Lorenzo, E., & Caamano, E. (2000). PV PUMPING ANALYTICAL DESIGN AND CHARACTERISTICS OF. *Solar Energy*, *68*(1), 49–56. http://doi.org/10.1016/S0038-092X(99)00050-X

Ngigi, S. N. (2002). Review of Irrigation Development in Kenya. *The Changing Face of Irrigation in Kenya: Opportunities for Anticipating Change in Eastern and Southern Africa.*, *2025*, 35–54.

NIB. (2016a). GALANA/ KULALU RANCH IRRIGATION PROJECT- GREEN REVOLUTION. Retrieved May 12, 2017, from https://www.nib.or.ke/91-nib/142-galana-kulalu-ranchirrigation-project-green-revolution

NIB. (2016b). Garissa County. Retrieved June 20, 2017, from https://www.nib.or.ke/projects/irrigation-projects-per-county?id=143

Ntengwe, F. W., Chikwa, M., & Witika, L. K. (2015). Evaluation Of Friction Losses In Pipes And Fittings Of Process Engineering Plants, *4*(10), 330–336.

Ofry, E., & Braunstein, A. (1983). The Loss of (Photovoltaic) Systems. *Transactions on Power Apparatus and Systems*, *PAS-102*(5), 1171–1175.

Ouachani, I., Rabhi, A., Yahyaoui, I., Tidhaf, B., & Tadeo, T. F. (2017). Renewable Energy Management Algorithm for a Water Pumping system. *Energy Procedia*, *111*(September 2016), 1030–1039. http://doi.org/10.1016/j.egypro.2017.03.266

Pereira, L. S., Cordery, I., & Iacovides, I. (2012). Improved indicators of water use performance and productivity for sustainable water conservation and saving. *Agricultural Water Management*, *108*, 39–51. http://doi.org/10.1016/j.agwat.2011.08.022

Posadillo, R., & Luque, R. L. (2008). Approaches for developing a sizing method for stand-alone PV systems with variable demand, *33*, 1037–1048. http://doi.org/10.1016/j.renene.2007.06.004

Pullenkav, T. (2013). Solar Water Pumping for Irrigation; Opportunities in Bihar, India. *GIZ(Indo-German Energy Programme - IGEN)*, 58pp.

Raturi, A. (2011). *Feasibility Study of Solar Water Pumping System*. Suva,Fiji.

Reddy, N. V. (2014). Design and optimization of solar powered irrigation system, *7*, 740–744.

RETScreen | Natural Resources Canada. (2017). Retrieved May 26, 2017, from http://www.nrcan.gc.ca/energy/software-tools/7465

Reuters. (2016, November 28). Solar irrigation cuts drought risk, emissions for Kenya’s farmers.

The Standard. Nairobi.

Reza, M., Hizam, H., Gomes, C., Amran, M., Ismael, M., & Hajighorbani, S. (2016). Power loss due to soiling on solar panel : A review. *Renewable and Sustainable Energy Reviews*, *59*, 1307–1316. http://doi.org/10.1016/j.rser.2016.01.044

Rezae, A., & Gholamian, S. A. (2013). Technical and Financial Analysis of Photovoltaic Water Pumping System for GORGAN , IRAN. *International Journal on Cybernetics and Informatics*, *2*(2). http://doi.org/10.5121/ijci.2013.2203

Richardson, J. F., & Coulson, J. M. (1999). *Chemical Engineering: Fluid Flow,Heat Transfer and Mass Transfer* (6th ed.). Oxford: Butterworth-Heinemann.

Rigollier, C., Bauer, O., Wald, L., Rigollier, C., Bauer, O., & Wald, L. (2009). On the clear sky model of the ESRA - European Solar Radiation Atlas with respect to the Heliosat method. *Solar Energy*, *68*, 33–48.

Shinde, V., & Wandre, S. S. (2016). Solar photovoltaic water pumping system for irrigation : A review Solar photovoltaic water pumping system for irrigation : A review. *African Journal of Agricultural Research*, *10*(May 2015), 2267–2273. http://doi.org/10.5897/AJAR2015.9879

Shrestha, P. D. J. N., Kumar Jha, D. A., & Karki, E. R. (2014). *Training Manual on Solar PV Pumping System*. Kathmandu.

Sidrch-de-Cardona, M., & Lopez, L. M. (1998). A simple model for sizing stand alone photovoltaic systems. *Solar Energy Materials and Solar Cells*, *55*, 199–214.

SolarAid. (2014). *Kenya Country Report 2014: SolarAid report of SunnyMoney activity in Kenya A welcome from Linda*. Nairobi,Kenya.

Solinc. (2016). The first solar product manufacturer in East Africa! Retrieved July 22, 2017, from www.solinc.co.ke/about-1/

Soto, W. De, Klein, S. A., & Beckman, W. A. (2006). Improvement and validation of a model for photovoltaic array performance. *Solar Energy*, *80*, 78–88. http://doi.org/10.1016/j.solener.2005.06.010

Turcotte, D., Ross, M., Sheriff, F., Blvd, L., & Tel, C. (2001). Photovoltaic Hybrid System Sizing and Simulation Tools: Status and Needs. In *PV Horizon: Workshop on Photovoltaic Hybrid Systems* (pp. 1–10). Quebec.

Twidell, J., & Weir, T. (n.d.). *Renewable Energy Resources* (2nd Editio). London and New York: Taylor and Francis Group.

UNESCO. (2013). *Agriculture, food and water. A contribution to the World Water Development Report*. http://doi.org/10.1016/B978-0-08-024618-5.50024-5

USDA. (2017). *World Agricultural Production*. Washington.

Wheeldon, S. (2016). Insight: The Rise of Solar-Powered Irrigation. Retrieved August 15, 2017, from https://poweringag.org/news-events/news/insight-rise-solar-powered-irrigation

Zanesco, I., Moechlecke, A., Medeiros, G. S., Severo, T. C., Eberhardt, D., Junior, S. L. R. S., & Zenzen, E. A. (2006). *Experimental Evaluation of an Analytic Method for Sizing Stand-Alone PV Systems*. Porto Alegre.

Zhou, W., Yang, H., & Fang, Z. (2007). A novel model for photovoltaic array performance prediction. *Applied Energy*, *84*, 1187–1198. http://doi.org/10.1016/j.apenergy.2007.04.006

APPENDICES

APPENDIX I

Average Climatic Conditions of Saretho. Garissa

Month	Relative Humidity (%)	Wind speed (m/s)	Rainfall (mm)	Irradiance (W/m^2)	Temperature (^0C)	Irradiation ($kWh/m^2/Day$)
January	46.19	3.64	26.68192	230	29.9	5.520
February	42.01	3.67	6.413083	240	30.92	5.760
March	47.58	3.74	11.09971	242	30.59	5.808
April	70.13	4.33	80.07008	229	27.16	5.496
May	66.37	5.56	34.8026	221	27.04	5.304
June	59.32	7.69	7.844807	200	26.2	4.800
July	57.16	7.93	8.40758	194	25.6	4.656
August	55.44	7.81	9.54616	213	26.21	5.112
September	54.5	7.88	12.51964	219	26.88	5.256
October	61.93	5.78	44.41295	241	27.21	5.784
November	75.01	2.36	81.68321	213	26.32	5.112
December	73.72	2.05	62.25451	218	26.39	5.232

APPENDIX II

Performance Characteristics of the PV Modules

TYPICAL PERFORMANCE CHARACTERISTICS (Nominal 12V Cells)

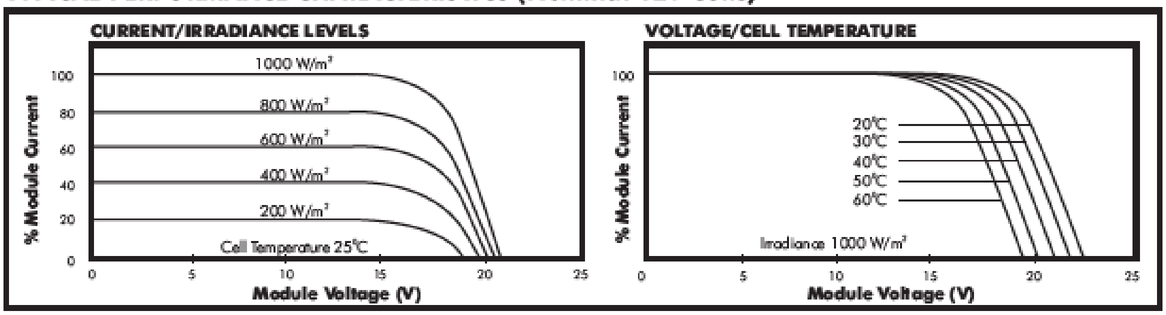

THERMAL CHARACTERISTICS

Nominal Operating Cell Temperature: 46+/-2°C
Temperature Coefficient Pmax.: -0.45%/°C
Temperature Coefficient Voc: -0.37%/°C
Temperature Coefficient Isc: 0.06%/°C

ELECTRICAL DATA

Model	Rated Power (W)	Nominal Voltage (V)	Peak Voltage (V)	Open Circuit Voltage (V)	Short Circuit Current (A)	Number of Cells
YL20	20	12	16.6	21.4	1.31	36
YL40	40	12	17.7	21.9	2.42	36
YL50	50	12	17.8	22.1	3.04	36
YL65	65	12	18	22	3.85	36
SW80	80	12	17.9	21.9	4.8	36
YL85	85	12	18.1	22.4	4.99	36
YL100	100	12	18.5	22.9	5.74	36
YL125	125	12	17.9	22.7	7.47	36
SW145	145	12	18	22.2	8.69	36
YL160	160	24	35.1	43.5	4.82	72
SW180	180	24	36	44.6	5.4	72
YL195	195	24	36.7	45.4	5.65	72
YL200	200	24	34.8	43.9	6.11	72
YL250	250	24	29.8	34.7	7.21	60
SW250	250	24	30.5	37.6	8.81	60

Data is given at Standard Test Conditions: Irradiance 1000W/m², spectrum AM 1.5 and 25°C cell temperature

APPENDIX

Performance Characteristics of the Diesel Generator

SPECIFICATIONS

Model	Voltage (V)	Output		Engine			Fuel tank capacity (litres)	Opera-ting Period (Hrs)	Starter
		Rated (KVA)	Max (KVA)	Model	Capacity (cc)	Max Power (HP)			
DG6000D	1x240	4.6	5.0	LA186FAFG	418	10	12.5	4	Electric
DG6000DS	1x240	4.6	5.0	LA186FAFG	418	10	16	5	Electric
DG12000DSM	1x240	10	11	LA290	954	20	53	14	Electric
DG12000DST	3x415	12.5	13.7	LA290	954	20	53	14	Electric

**Acoustic Set with AMF, noise level: 70dBA@7m*

DERATING: Given outputs are sea level rating. Sets should be derated at 1% for every 100m higher than 100m above sea level, and 2% for every 5°C temperature above 20°C

ELECTRICAL DATA

Alternator: Brushless, self exciting, 2 pole
Voltage Regulator: AVR
Speed: 3000rpm
Power Factor: 1
Direct Current: 12V/8.3A

DIMENSIONS AND WEIGHTS

Model	L (mm)	W(mm)	H(mm)	Weight (kg)
DG6000D	740	475	590	95
DG6000DS	900	520	700	150
DG12000DSM	1150	670	940	295
DG12000DST				

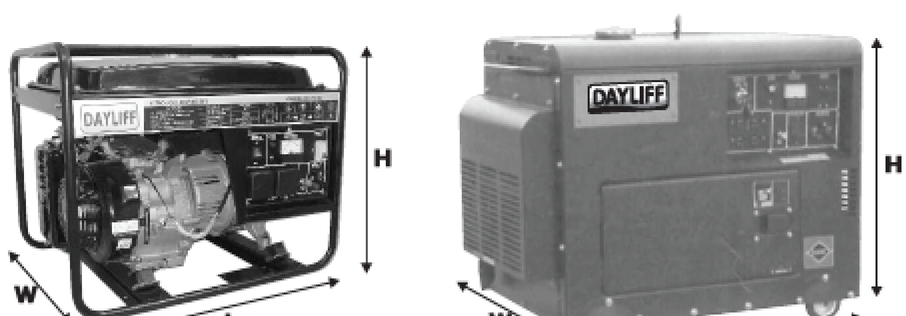

APPENDIX III

Performance Characteristics of the Solar Water Pump

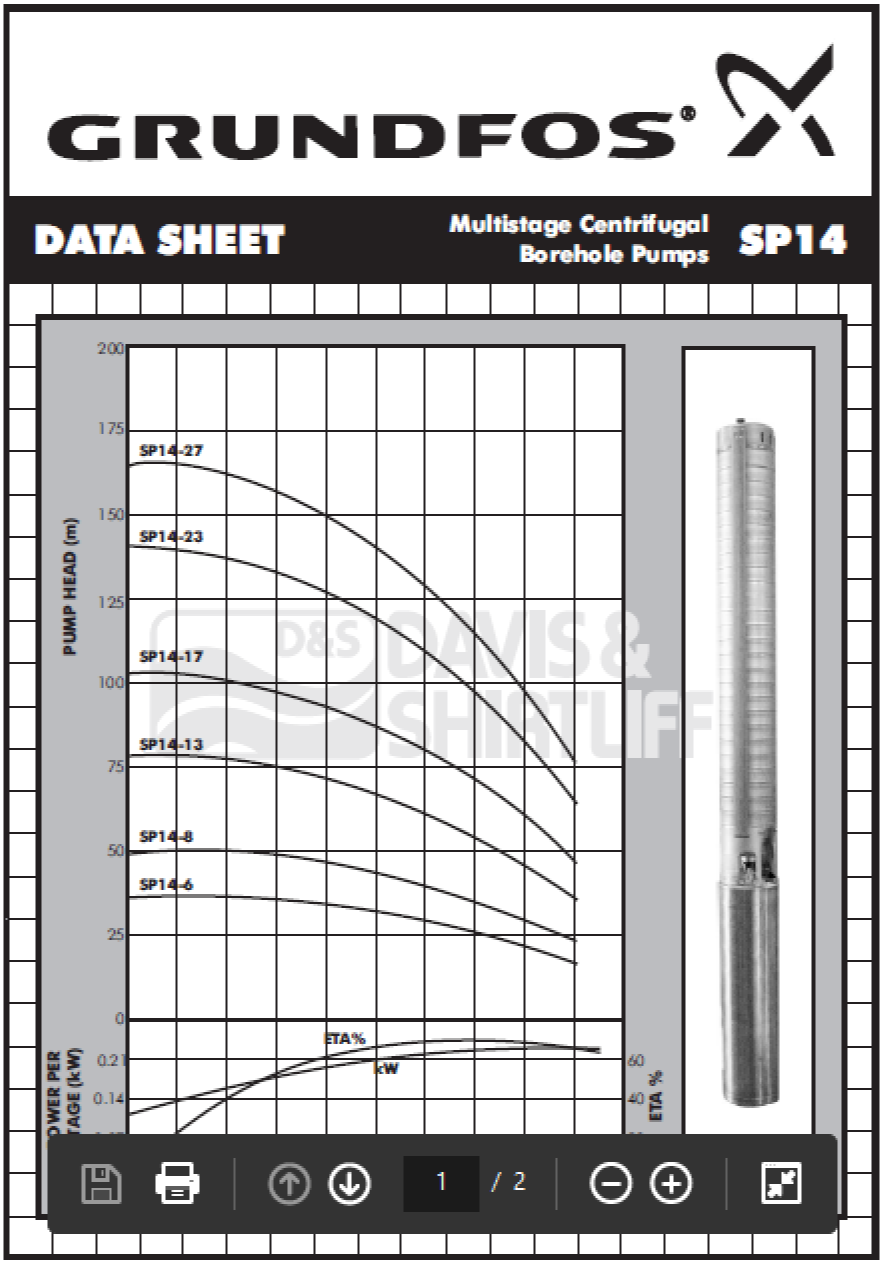

APPENDIX IV

Quotation for Prices of SPIS and SPIS components

DAVIS & SHIRTLIFF
know H2Ow through experience

DAVIS & SHIRTLIFF LTD
Dundori Rd, Industrial Area
PO Box 41762-00100 NAIROBI KENYA
Tel: (+254 20) 6968 000, 558335
d&s@dayliff.com
www.davisandshirtliff.com

QUOTATION

REF	**311205/WT RI**
DATE	**25 Jul 2017**

TO: HILLARY KIPRONO
kipronohillary11@gmail.com

SUBJECT: QUOTATION FOR SUPPLY OF ITEMS
WATER TREATMENT RETAIL JOB

No.	DESCRIPTION	QTY	VAT	PRICE	AMOUNT
1	LORENTZ PS4000 C-SJ8-15 pump C/W CONTROLLER	1	16%	290,000.00	290,000.00
2	DAYLIFF 200W 24VDC POLYCRYSTALLINE SOLAR MODULE	1	0%	16,000.00	16,000.00
3	GRUNDFOS SP 14-08 2.2kW 1PH PUMP COMPLETE	1	16%	218,000.00	218,000.00
4	DAYLIFF DG6000DS 4.5kVA SILENT GENSET	1	0%	142,000.00	142,000.00
			SUB-TOTAL	KES	666,000.00
			LESS DISCOUNT	KES	112,800.00
			NET	KES	553,200.00
			ADD VAT	KES	66,768.00
			TOTAL	**KES**	**619,968.00**

DELIVERY AVAILABLE EX-STOCK SUBJECT TO PRIOR SALE
VALIDITY SUBJECT TO CONFIRMATION AT DATE OF ORDER
PAYMENT FULL PAYMENT
WARRANTY STANDARD D&S WARRANTY TERMS APPLY